Electronic Supplementary Material (ESI) for ChemComm.

Supporting Information

Synergistic repulsive interactions trigger pathway complexity

Ingo Helmers,[a] Maximilian Niehues,[a] Kalathil K. Kartha,[a] Bart Jan Ravoo,[a] and Gustavo Fernández*[a]

[a] Organisch-Chemisches Institut, Westfälische Wilhelms-Universität Münster, Corrensstrasse 40, 48149 Münster (Germany), E-mail: fernandg@uni-muenster.de

Table of Contents

Experimental Procedures

Materials and Methods

Chemical and Reagents: All chemicals were purchased from Sigma-Aldrich (St. Louis, MO, USA), TCI Europe N.V. (Tokyo, JP) or Alfa Aesar (Ward Hill, MA, USA), with minimum analytical grade quality and used without further purification unless otherwise stated. Dichloromethane was pre-dried over $CaCl_2$ and then distilled over P_2O_5 under argon atmosphere. Silica gel was used for column chromatography, unless otherwise indicated.

Column chromatography. Preparative column chromatography was conducted in self-packed glass columns of different sizes with silica gel (particle size: 40 – 60 µm, *Merck*). Dichloromethane and methanol were distilled before usage.

NMR spectroscopy: ^{1}H and ^{13}C NMR spectra were recorded at 298 K on Avance II 300 and Avance II 400 from Bruker for routine experiments using tetramethylsilane (TMS) as internal reference, and DD2 500 and DD2 600 from Agilent for characterization purposes. Multiplicities for proton signals are abbreviated as s, d, t, q and m for singlet, doublet, triplet, quadruplet and multiplet respectively.

Mass spectrometry: ESI mass spectra were measured using a Bruker MicrOToF system.

UV/Vis and fluorescence spectroscopy: UV/Vis absorption spectra were recorded on a Jasco V-770 or Jasco V-750 spectrophotometers, both equipped with peltier cells and Julabo F250 water circulation units. Fluorescence spectra were recorded on a Jasco FP-8500 spectrofluorimeter equipped with the same water circulation unit.

Transmission electron microscopy (TEM) was performed using a Titan Themis G3 300 TEM (*FEI*). For all measurements, the microscope was operated at 300 kV with an extraction voltage of 3.45 kV for the field emission gun. TEM measurement data was analyzed with Image J version 1.52h (*National Institutes of Health*, USA, Java 1.8.0_66).

FTIR spectroscopy was carried out using a JASCO-FTIR-6800 equipped with a CaF2 cell with a path length of 0.1 mm.

Sample preparation method: Samples were dissolved in a suitable co-solvent (propane-1,2-diol, acetone or THF) and subsequently water was added to induce aggregation. Prepared solutions were used for UV-Vis, NMR, emission spectroscopy and conventional TEM. For TEM measurements sample preparation was performed by incubation of a glow-discharged carbon coated copper grid (S162, *Plano*) with 5 µL of the prepared aggregate solution for 1 min and gentle blotting with filter paper. The sample was stained with 5 µL of 0.1% (w/w) aqueous uranyl acetate (UA) for 30 s and again gently blotted with filter paper.

Synthesis and characterization of 1-4

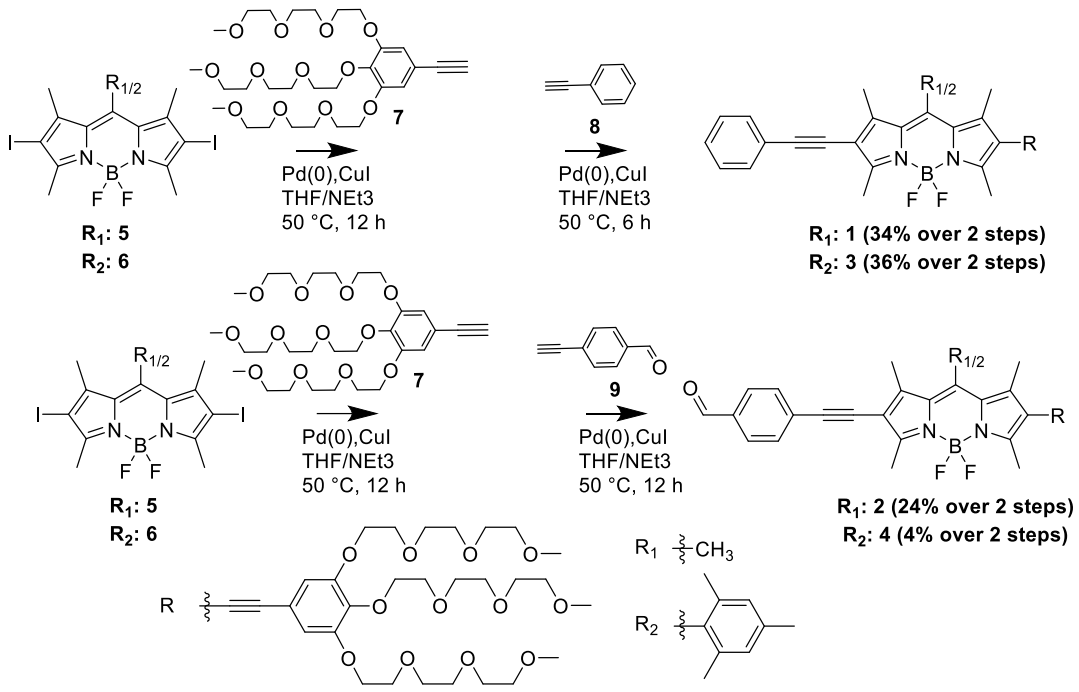

5,5-difluoro-2,8-diiodo-1,3,7,9,10-pentamethyl-5*H*-4λ^4,5 λ^4-dipyrrolo[1,2-c:2',1'-f][1,3,2]diazaborinine (**5**),[1] 5,5-difluoro-2,8-diiodo-10-mesityl-1,3,7,9-tetramethyl-5*H*-4 λ^4,5 λ^4-dipyrrolo[1,2-c:2',1'-f][1,3,2]diazaborinine (**6**),[2] 4-ethynylbenzaldehyde (**9**)[3] and 5-ethynyl-1,2,3-tris(2-(2-(2-methoxyethoxy)ethoxy)ethoxy)-benzene (**7**)[4] were prepared following reported synthetic procedures and showed identical spectroscopic properties to those reported therein.

Synthesis of 5,5-difluoro-1,3,7,9,10-pentamethyl-2-(phenylethynyl)-8-((3,4,5-tris(2-(2-(2-methoxyethoxy)ethoxy)ethoxy)phenyl)ethynyl)-5H-5λ^4,6λ^4-dipyrrolo[1,2-c:2',1'-f][1,3,2]diazaborinine (1)

5,5-difluoro-2,8-diiodo-1,3,7,9,10-pentamethyl-5*H*-4λ^4,5λ^4-dipyrrolo[1,2-c:2',1'-f][1,3,2] diazaborinin (**5**, 0.12 g, 0.24 mmol, 1 Äq.), $(PPh_3)_4Pd$ (8 mg, 0.01 mmol, 0.05 Äq.) and CuI (2 mg, 0.01 mmol, 0.05 Äq.) in THF (15 mL) and NEt_3 (5 mL) was heated to 50 °C and 5-ethinyl-1,2,3-*tris*(2-(2-(2-methoxyethoxy)ethoxy)ethoxy)benzene (**7**, 0.14 g, 0.24 mmol, 1 Äq.) in THF (20 mL) was added over a time span of 5 hours. After addition the reaction mixture was stirred for additional 12 hours at 50 °C. Phenylacetylene (**8**, 0.07 g, 0.71 mmol, 3 Äq.) was added and stirred at 50 °C for further 6 hours. The solvent was removed and the crude product purified by column chromatography running an increasing CH_2Cl_2/MeOH gradient (1%-5%) from CH_2Cl_2.
Yield = 70 mg (0.08 mmol, 34%) of a dark violet solid.

Characterization:

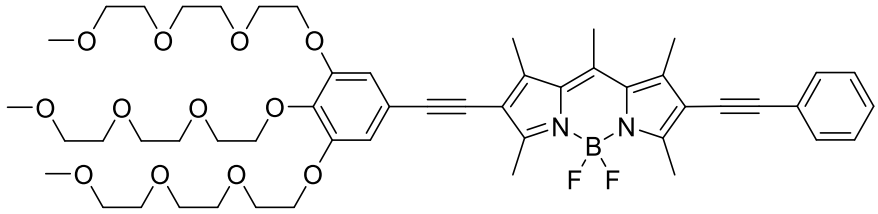

Chemical Formula: $C_{51}H_{67}BF_2N_2O_{12}$
Exact Mass: 948,4755
Molecular Weight: 948,9058

^{1}H NMR (500 MHz, Methylene Chloride-d_2):
δ (in ppm) = 7.56 (dd, *J* = 7.9, 1.7 Hz, 2H), 7.44 – 7.33 (m, 3H), 6.81 (s, 2H), 4.31 – 4.12 (m, 6H), 3.93 – 3.58 (m, 24H), 3.57 – 3.48 (m, 6H), 3.36 (m, *J* = 4.1 Hz, 9H), 2.71 (s, 3H), 2.68 (m, 6H), 2.62 (m, 6H).

^{13}C NMR (126 MHz, Methylene Chloride-d_2):
δ (in ppm) = δ 156.5, 156.4, 152.6, 143.0, 142.1, 139.2, 131.2, 128.4, 128.2, 123.4, 118.2, 115.9, 110.6, 96.3, 96.3, 81.6, 80.6, 72.5, 71.9, 70.8, 70.6, 70.5, 70.4, 69.6, 68.8, 58.6, 31.9, 29.7, 29.3, 22.7, 17.3, 17.0, 15.9, 15.9, 15.7, 13.9, 13.4, 13.3.

ESI-MS (TOF)**:**
m/z 971.4636 $[M+Na]^+$, calculated for $C_{51}H_{67}N_2O_{12}BF_2Na$: 971.4647

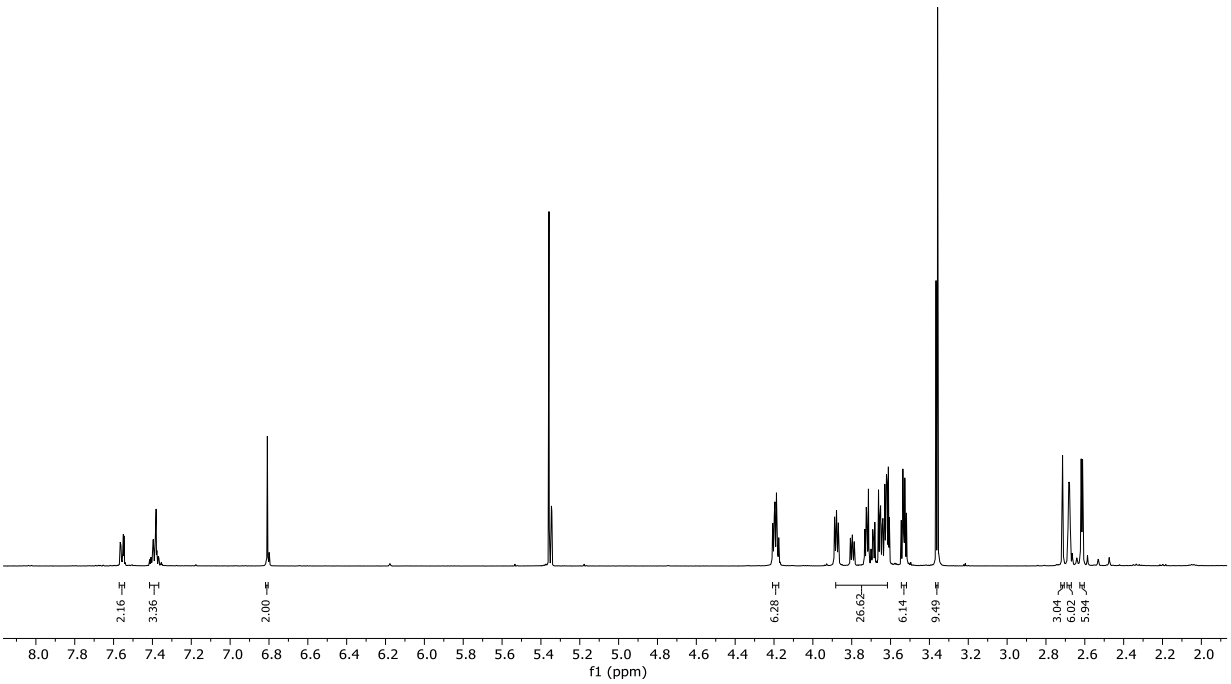

Figure S1. ^{1}H NMR (500 MHz, Methylene Chloride-d_2, 298 K) of **1**.

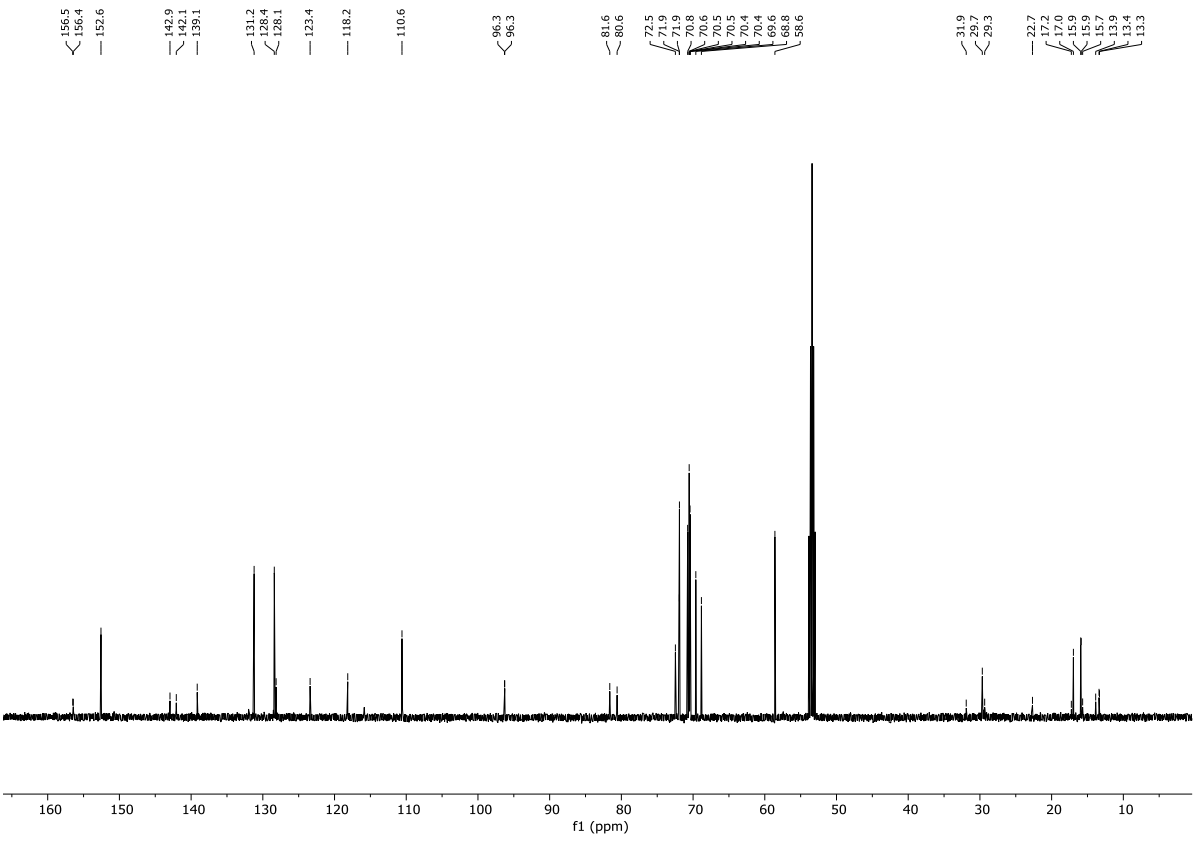

Figure S2. ^{13}C NMR (126 MHz, Methylene Chloride-d_2, 298 K) of compound **1**.

Synthesis of 4-((5,5-difluoro-1,3,7,9,10-pentamethyl-8-((3,4,5-tris(2-(2-(2-methoxyethoxy)ethoxy)ethoxy)phenyl)ethynyl)-5H-4λ^4,5λ^4-dipyrrolo[1,2-c:2',1'-f][1,3,2]diazaborinin-2-yl)ethynyl)benzaldehyde (2)

5,5-difluoro-2,8-diiodo-1,3,7,9,10-pentamethyl-5H-4λ^4,5λ^4-dipyrrolo[1,2-c:2',1'-f][1,3,2] diazaborinine (**5**, 1.97 g, 3.83 mmol, 1 eq), $(PPh_3)_4Pd$ (0.13 g, 0.12 mmol, 0.05 eq) and CuI (21.0 mg, 0.12 mmol, 0.05 eq) were dissolved after three vacuum-argon cycles in anhydrous THF (60 mL) and NEt_3 (20 mL). The reaction mixture was heated to 50 °C and 4-ethynylbenzaldehyde (**9,** 0.50 g, 3.83 mmol, 1 eq) dissolved in THF (200 mL) was added dropwise over the course of 5 hours to the solution and stirred for additional 12 h at 50 °C. The mixture was concentrated and the crude product purified by silica gel column chromatography using a gradient from *n*-Pentane/DCM (1/1, (*v*/*v*)) to DCM as eluent. The crude product (0.68 g, 1.32 mmol) was used without further purification for the next reaction.
The raw product (0.68 g, 1.32 mmol, 1 eq), $(PPh_3)_4Pd$ (76.5 mg, 66.2 µmol, 0.05 eq) and CuI (12.6 mg, 66.2 µmol, 0.05 eq) were dissolved after three vacuum-argon cycles in anhydrous THF (18 mL) and NEt_3 (2 mL). The reaction mixture was heated to 50 °C and 5-ethynyl-1,2,3-tris(2-(2-(2-methoxyethoxy)ethoxy)ethoxy)benzene (**7,** 0.67 g, 1.19 mmol, 0.9 eq) was added. The solution was stirred for 12 h. The mixture was concentrated and the crude product purified by silica gel column chromatography using a gradient from DCM to DCM/MeOH (5%) as eluent
Yield: 0.90 g (0.92 mmol, 24%) of a dark purple solid.

Characterization:

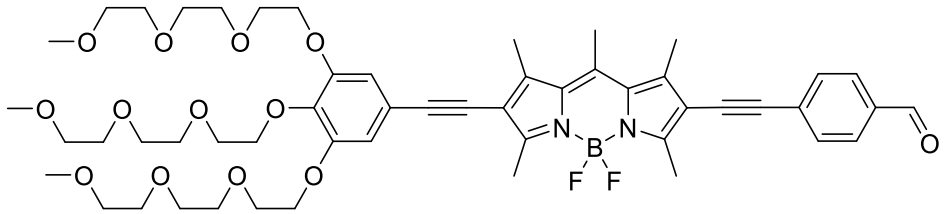

Chemical Formula: $C_{52}H_{67}BF_2N_2O_{13}$
Exact Mass: 976.4704
Molecular Weight: 976.9158

^{1}H NMR (400 MHz, $CDCl_3$):
δ (in ppm) = 9.92 (s, 1H-ALD), 7.77 (d, *J* = 8.4 Hz, 2H-Ar), 7.55 (d, *J* = 8.2 Hz, 2H-Ar), 6.67 (s, 2H-Ar-TEG), 4.11 (m, 6H-TEG), 3.94 – 3.54 (m, 24H-TEG), 3.48 (m, 6H-TEG), 3.30 (m, 9H-TEG), 2.74 – 2.52 (m, 9H-BODIPY), 2.48 (m, 6H-BODIPY).

^{13}C NMR (101 MHz, $CDCl_3$):
δ (in ppm) = 191.5, 157.7, 156.4, 152.6, 142.7, 142.6, 141.9, 139.4, 135.2, 132.4, 131.9, 131.7, 129.9, 129.7, 118.2, 116.6, 115.1, 111.1, 96.7, 95.8, 86.5, 80.7, 72.6, 72.0, 70.9, 70.8, 70.8, 70.7, 70.6, 70.6, 69.7, 69.0, 59.1, 17.1, 16.4, 16.2, 13.8, 13.7.

ESI-MS (TOF)**:**
m/*z* 999.46079 $[M+Na]^+$, calculated for $C_{52}H_{67}N_2O_{13}BF_2Na$: 999.46053

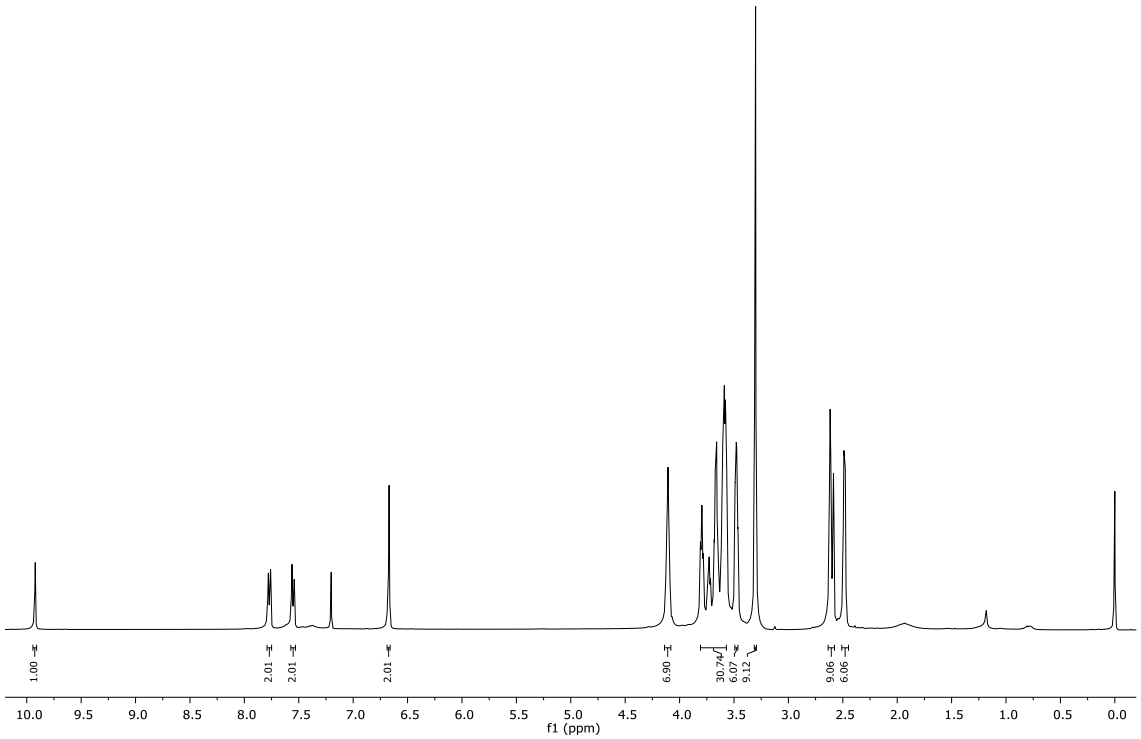

Figure S3. ^{1}H NMR (400 MHz, $CDCl_3$, 298 K) of **2**.

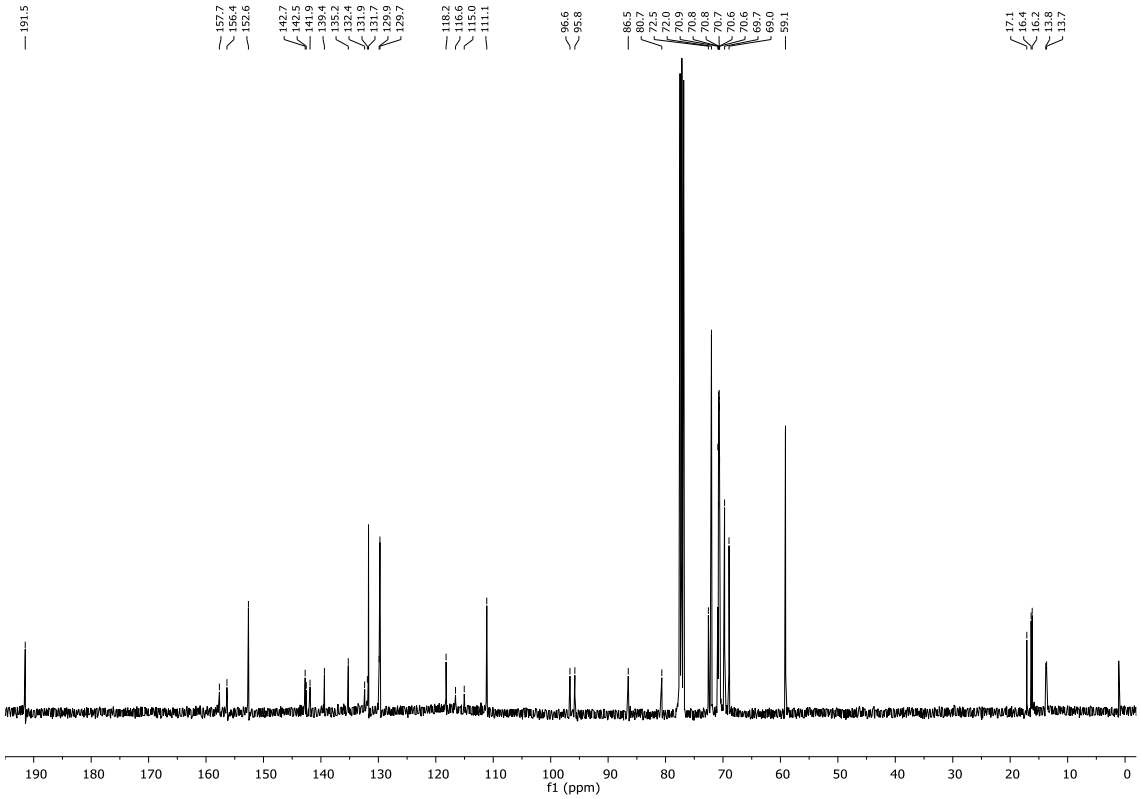

Figure S4. ^{13}C NMR (101 MHz, $CDCl_3$, 298 K) of compound **2**.

Synthesis of 5,5-difluoro-10-mesityl-1,3,7,9-tetramethyl-2-(phenylethynyl)-8-((3,4,5-tris(2-(2-(2-methoxyethoxy)ethoxy)ethoxy)phenyl)ethynyl)-5H-5λ^4,6λ^4-dipyrrolo[1,2-c:2',1'-f][1,3,2]diazaborinine (3)

5,5-difluoro-2,8-diiodo-10-mesityl-1,3,7,9-tetramethyl-5*H*-4λ^4,5λ^4-dipyrrolo[1,2-c:2',1'-f][1,3,2]diazaborinine (**6**, 0.52 g, 0.85 mmol, 1 eq.), $(PPh_3)_4Pd$ (30 mg, 0.04 mmol, 0.05 eq.) and CuI (9.0 mg, 0.04 mmol, 0.05 eq.) in THF (20 mL) and NEt_3 (20 mL) was heated to 50 °C and 5-ethynyl-1,2,3-*tris*(2-(2-(2-methoxyethoxy)ethoxy)ethoxy)benzene (**7**, 0.50 g, 0.85 mmol, 1 eq.) in THF (20 mL) was added dropwise over a time span of 5 hours. After addition the reaction mixture was stirred for additional 12 hours at 50 °C. Phenylacetylene (**8**, 0.17 g, 1.70 mmol, 2 Äq.) was added and stirred at 50 °C for further 6 hours. The solvent was removed and the crude product purified by column chromatography running an increasing CH_2Cl_2/MeOH gradient (1%-5%) from CH_2Cl_2.
Yield = 0.33 g (0.30 mmol, 36%) of a dark violet solid.

Characterization:

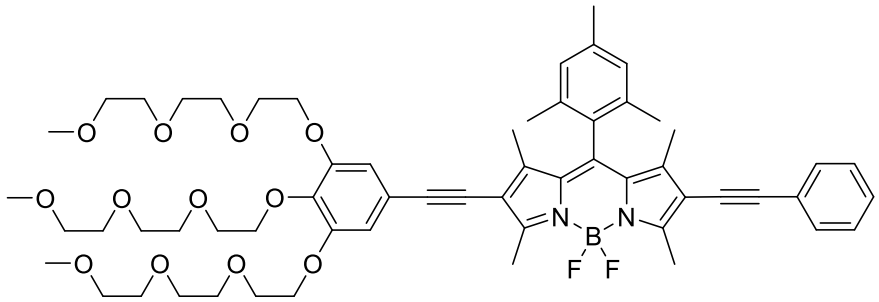

Chemical Formula: $C_{59}H_{75}BF_2N_2O_{12}$
Exact Mass: 1052,5381
Molecular Weight: 1053,0578

^{1}H NMR (600 MHz, $CDCl_3$):
δ (in ppm) = 7.49 – 7.42 (m, 2H), 7.37 – 7.29 (m, 3H), 6.99 (s, 2H), 6.69 (s, 2H), 4.15 (m, 6H), 3.90 – 3.58 (m, 24 H), 3.57 – 3.51 (m, 6H), 3.36 (m, 9H), 2.71 (m, 6H), 2.36 (s, 3H), 2.10 (s, 6H), 1.53 (m, 6H).

^{13}C NMR (151 MHz, $CDCl_3$):
δ (in ppm) = δ 158.4, 158.2, 152.6, 143.4, 143.3, 142.8, 139.4, 139.2, 134.9, 131.5, 130.7, 129.3, 128.5, 128.3, 123.6, 118.4, 115.9, 111.2, 96.5, 96.4, 81.7, 80.9, 72.6, 72.1, 71.0, 70.8, 70.7, 69.8, 69.0, 59.2, 59.1, 53.6, 34.3, 29.8, 22.5, 21.4, 19.6, 14.2, 13.9, 13.8, 12.6, 12.5.

ESI-MS (TOF)**:**
m/z 1075.5275 $[M+Na]^+$, calculated for $C_{59}H_{75}N_2O_{12}BF_2Na$: 1075.5283

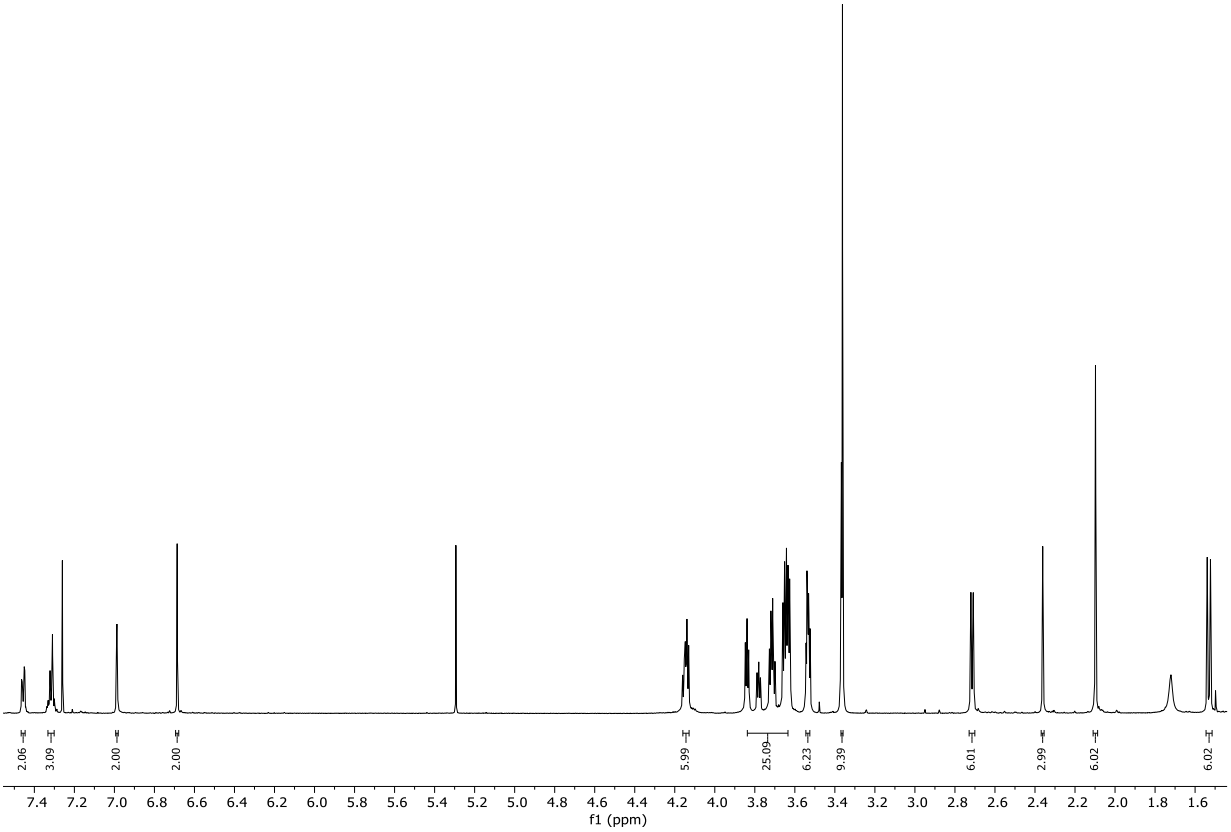

Figure S5. ^{1}H NMR (600 MHz, Methylene Chloride-d_2, 298 K) of **3**.

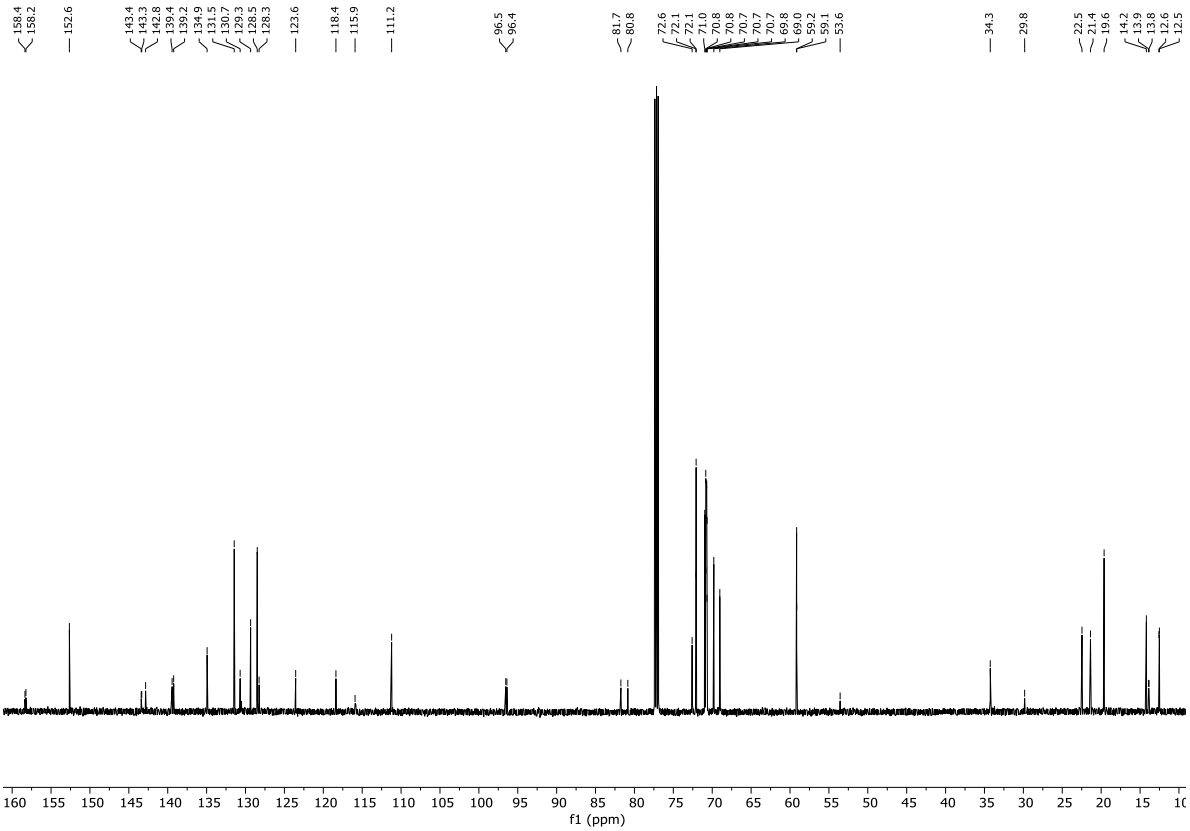

Figure S6. ^{13}C NMR (151 MHz, Methylene Chloride-d_2, 298 K) of compound **3**.

Synthesis of 4-((5,5-Difluoro-8-iodo-10-mesityl-1,3,7,9-tetramethyl-5H-5λ4,6λ4-dipyrrolo[1,2-c:2',1'-f][1,3,2]diazaborinin-2-yl)ethynyl)benzaldehyde (10)

5,5-difluoro-2,8-diiodo-10-mesityl-1,3,7,9-tetramethyl-5*H*-4λ^4,5λ^4-dipyrrolo[1,2-c:2',1'-f][1,3,2]diazaborinine (**6**, 1.19 g, 1.93 mmol), $Pd(Ph_3)_4$ (111 mg, 100 µmol) and CuI (19 mg, 100 µmol) were dissolved in NEt_3/THF (10 mL/10 mL) under argon atmosphere and the mixture was heated up to 50 °C. A solution of 4-ethynylbenzaldehyde (**9**, 250 mg, 1.93 mmol) in THF (100 mL) was added dropwise over two hours. After stirring overnight, the solvent was removed under reduced pressure and the crude mixture was purified by column chromatography (n-pentane/ CH_2Cl_2 4:1 to 1:1)
Yield: 150 mg (0.24 mmol, 12 %) of a red-brown solid.

Characterization:

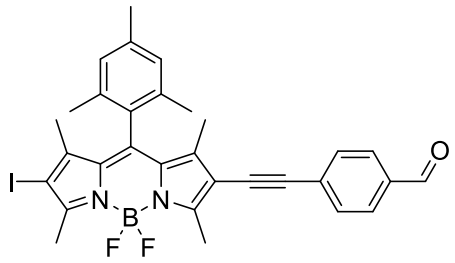

Chemical Formula: $C_{31}H_{28}BF_2IN_2O$
Exact Mass: 620.1307
Molecular Weight: 620.2893

^{1}H NMR (300 MHz, $CDCl_3$):
δ (in ppm) = 10.00 (s, 1H), 7.84 (d, *J* = 8.3 Hz, 2H), 7.58 (d, *J* = 8.3 Hz, 2H), 6.99 (s, 2H), 2.70 (d, *J* = 14.1 Hz, 6H), 2.37 (s, 3H), 2.08 (s, 6H), 1.53 (s, 3H), 1.44 (s, 3H).

^{13}C NMR (101 MHz, $CDCl_3$):
δ (in ppm) = 191.5, 158.0, 157.4, 145.0, 144.0, 142.7, 139.4, 135.3, 134.9, 131.8, 131.6, 130.7, 129.9, 129.8, 129.5, 95.8, 86.4, 21.4, 19.7, 16.2, 16.0, 13.9, 12.6.

ESI-MS (TOF)**:**
m/*z* 643.1199 $[M+H]^+$, calculated for $C_{23}H_{22}N_3O_6$: 643.1200

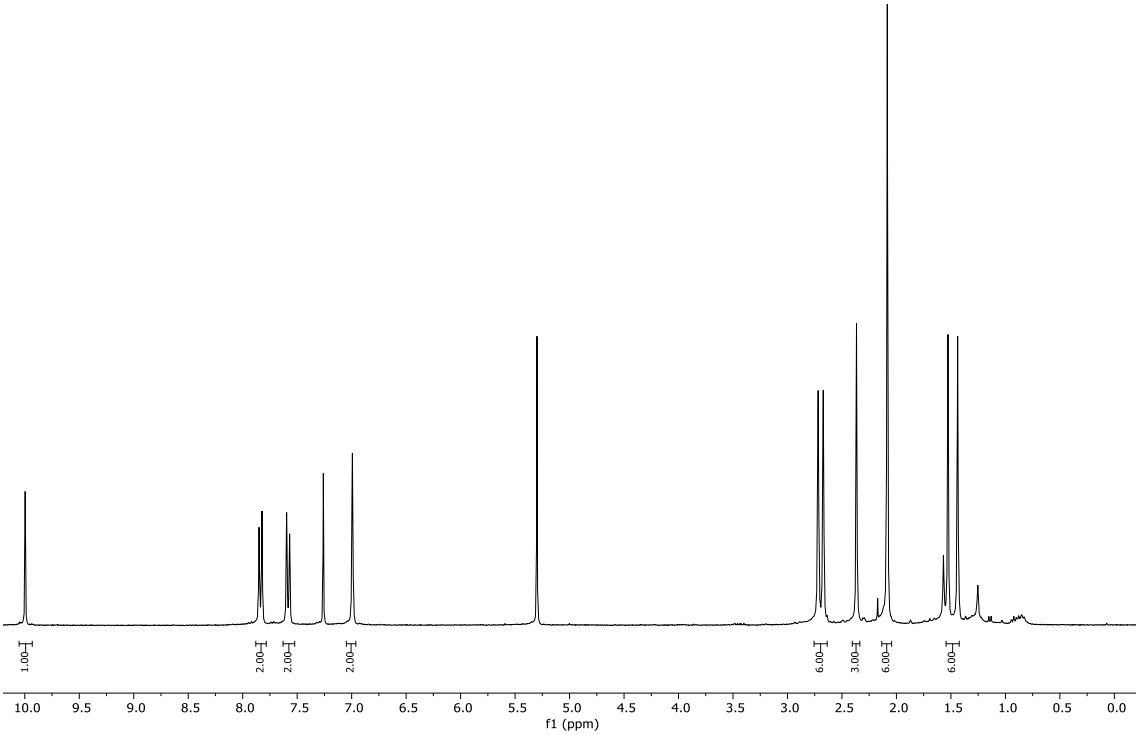

Figure S7. ^{1}H NMR (300 MHz, $CDCl_3$, 298 K) of **10**.

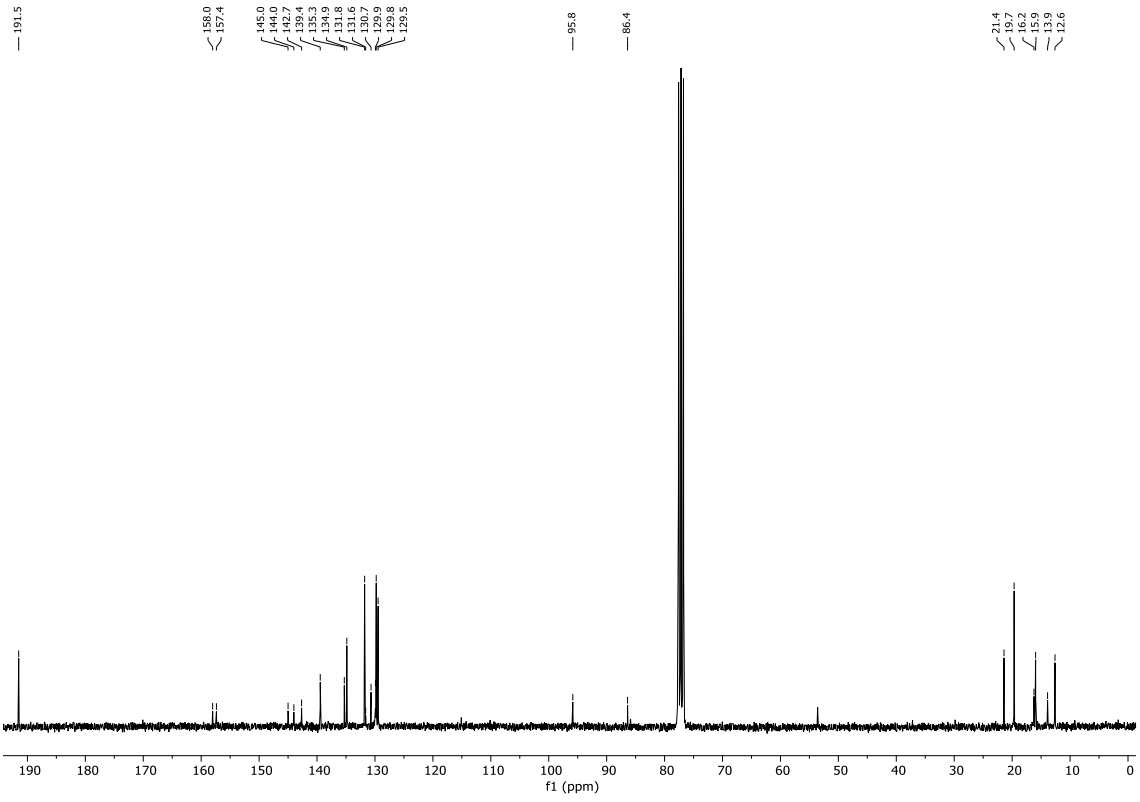

Figure S8. ^{13}C NMR (101 MHz, $CDCl_3$, 298 K) of compound **10**.

Synthesis of 4-((5,5-Difluoro-10-mesityl-1,3,7,9-tetramethyl-8-((3,4,5-tris(2-(2-(2-methoxyethoxy)ethoxy)ethoxy)phenyl)ethynyl)-5*H*-5λ^4,6λ^4-dipyrrolo[1,2 c:2',1' f][1,3,2]diazaborinin-2-yl)ethynyl)benzaldehyde (4)

To a mixture of **10** (290 mg, 470 µmol), $Pd(Ph_3)_4$ (27 mg, 20.0 µmol) and CuI (5 mg, 0.02 mmol) in NEt_3/THF (5 mL/20 mL) 5-ethynyl-1,2,3-tris(2-(2-(2-methoxyethoxy)ethoxy)ethoxy)benzene (**7**, 221 mg, 380 µmol) was added. The reaction mixture was stirred at 50 °C overnight and the solvent was removed under reduced pressure. The crude product was purified by column chromatography running an increasing CH_2Cl_2/MeOH gradient (1%-5%) from CH_2Cl_2.
Yield = 160 mg (0.15 mmol, 32%) of a dark blue solid.

Characterization:

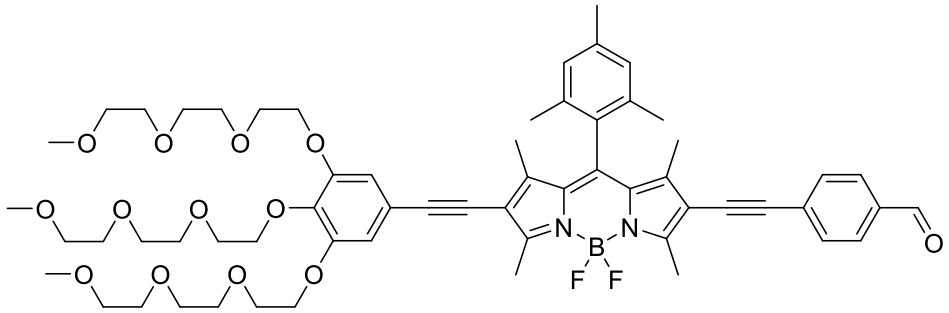

Chemical Formula: $C_{60}H_{75}BF_2N_2O_{13}$
Exact Mass: 1080,5330
Molecular Weight: 1081,0678

^{1}H NMR (300 MHz, $CDCl_3$):
δ (in ppm) = 9.99 (s, 1H), 7.90–7.76 (m, 2H), 7.58 (d, J = 8.2 Hz, 2H), 6.99 (s, 2H), 6.68 (s, 2H), 4.20–4.05 (m, 6H), 3.90–3.48 (m, 30H), 3.36 (d, J = 1.4 Hz, 9H), 2.72 (d, J = 2.6 Hz, 6H), 2.36 (s, 3H), 2.09 (s, 6H), 1.54 (d, J = 4.8 Hz, 6H)

^{13}C NMR (101 MHz, $CDCl_3$):
δ (in ppm) = 191.5, 159.2, 157.9, 152.6, 144.0, 143.4, 143.1, 139.4, 139.3, 135.2, 134.8, 131.7, 130.9, 130.5, 130.4, 129.9, 129.8, 129.4, 118.2, 116.3, 114.8, 111.1, 96.7, 95.8, 86.5, 80.6, 77.4, 72.5, 72.0, 72.0, 70.9, 70.8, 70.7, 70.6, 69.7, 68.9, 59.1, 29.8, 21.4, 19.6, 14.0, 13.8, 12.7, 12.5

ESI-MS (TOF)**:**
m/z 1103.522 $[M+Na]^+$, calculated for $C_{75}H_{86}BF_2N_5O_{19}Na$: 1103.522

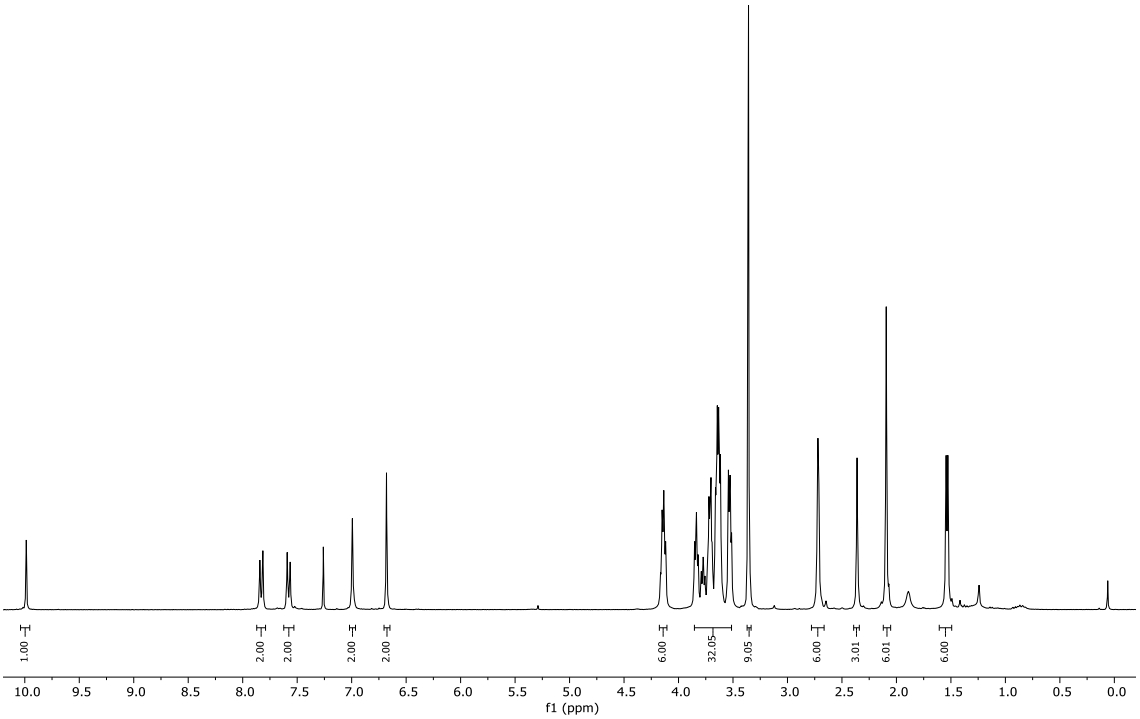

Figure S9. ^{1}H NMR (300 MHz, $CDCl_3$, 298 K) of **4**.

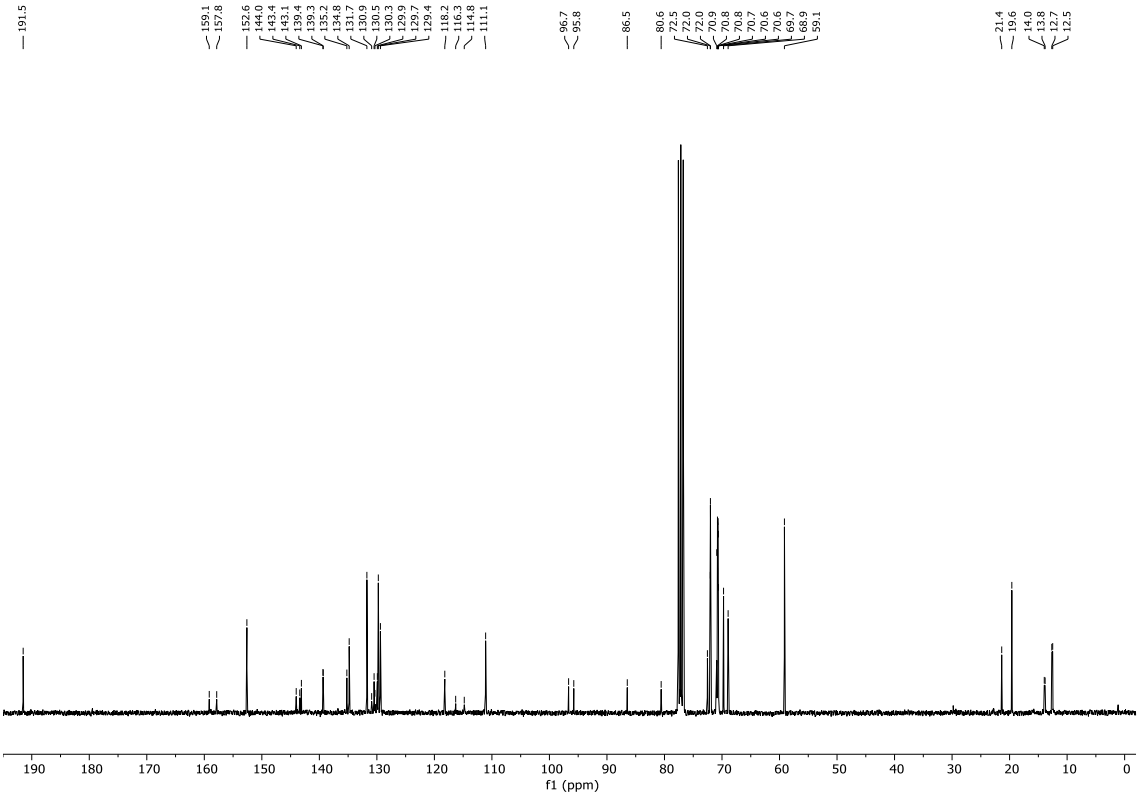

Figure S10. ^{13}C NMR (101 MHz, $CDCl_3$, 298 K) of compound **4**.

Results and Discussion

Nucleation-Elongation model for Cooperative Supramolecular Polymerizations

The equilibrium between the monomeric and supramolecular species can be described in a cooperative process with the *Nucleation-Elongation model* which is developed by Ten Eikelder, Markvoort and Meijer [5-6] This model is used to describe the aggregation **2** and **4** which exhibit a non-sigmoidal cooling curve as shown in UV-Vis temperature-dependent experiments. The model extends nucleation-elongation based equilibrium models for growth of supramolecular homopolymers to the case of two monomer and aggregate types and can be applied to symmetric supramolecular copolymerizations, as well as to the more general case of nonsymmetric supramolecular copolymerizations.

In a cooperative process, the polymerization occurs by a nucleation step, to a nucleus size assumed of B, and a following elongation step. The values T_e, $\Delta H°_{nucl}$, $\Delta H°$ and $\Delta S°$ can be determined by a non-linear least-square analysis of the experimental melting curves. The equilibrium constants associated with the nucleation and elongation phases can be calculated using equations **1** and **2**:

Nucleation step: $K_n = e^{\left(\frac{-((\Delta H^o - \Delta H^o_{NP}) - T\Delta S^o)}{RT}\right)}$ $(\mathbf{1})$

Elongation step: $K = e^{\left(\frac{-(\Delta H^o - T\Delta S^o)}{RT}\right)}$ $(\mathbf{2})$

And the cooperativity factor (σ) is given by:

$$\sigma = \frac{K_n}{K_e} = e^{\left(\frac{\Delta H^o_{NP}}{RT}\right)} \qquad (\mathbf{3})$$

Fluorescence Quantum Yields

The fluorescence quantum yields for **1**-**4** were calculated using Rhodamine 101 (MeOH) as standard (Φ_{ref} = 1.0) and using the following equation:

$$\Phi = \Phi_{ref} \frac{A_r\, I}{A\, I_f}$$

A: Absorption (set under 0.1) for reference and sample
I: Integral of emission-peak for reference and sample

Table S1. Fluorescence Quantum Yields of **1**-**4** in different solvents

	Solvent	ϕ_F
1	DCM	32.5%
2	DCM	44.1%
3	DCM	36.1%
4	DCM	26.7%
1	H_2O	0.1%
2	H_2O	0.8%
3	H_2O	1.2%
4A	H_2O	0.6%
4B	H_2O	0.4%

Thermodynamic Parameters

The thermodynamic parameters for **2,4** (**Table S1**) were obtained by fitting the respective experimental data to the nucleation-elongation model

Table S2. Thermodynamic parameters of supramolecular polymerization of **2**, **4A** and **4B**.

	c / μM	ΔH_0 / kJ	ΔS_0 / kJ	ΔH_{NP} / kJ	T_E / K	ΔG_{298} / kJ	K_{el}	K_{nucl}	σ
2	10	-56.8	-0.08	-15.6	317.0	-30.2	50004.0	134.9	0.0027
2	20	-60.7	-0.09	-17.3	324.5	-33.5	100004.3	162.7	0.0016
2	30	-63.4	-0.11	-11.8	321.3	-30.4	33333.6	405.8	0.0112
4A	10	-46.9	-0.05	-14.8	349.5	-32.2	100011.2	406.3	0.004
4A	20	-46.4	-0.04	-17.1	353.9	-34.1	50002.2	148.6	0.002
4A	30	-39.0	-0.02	-22.1	358.2	-32.4	33333.8	19.8	5.9×10^{-4}
4B	10	-71.9	-0.12	-15.2	331.3	-35.7	100006.3	398.6	0.004
4B	20	-88.5	-0.18	-14.1	331.5	-34.7	33333.2	345.6	0.006
4B	30	-121.2	-0.27	-12.8	333.0	-39.5	50000.8	496.9	0.010

Supplementary Figures

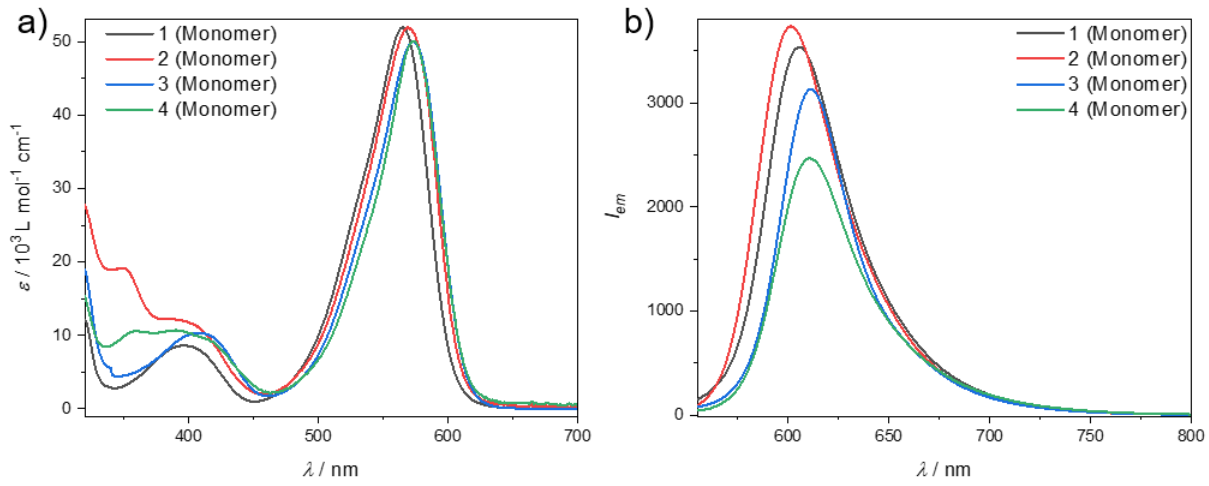

Figure S11. UV Vis (a) and emission (b) spectra of **1-4** in a monomeric (DCM) state at 298 K (*c* = 20 μM). Excitation wavelength λ = 530 nm was applied for all measurements.

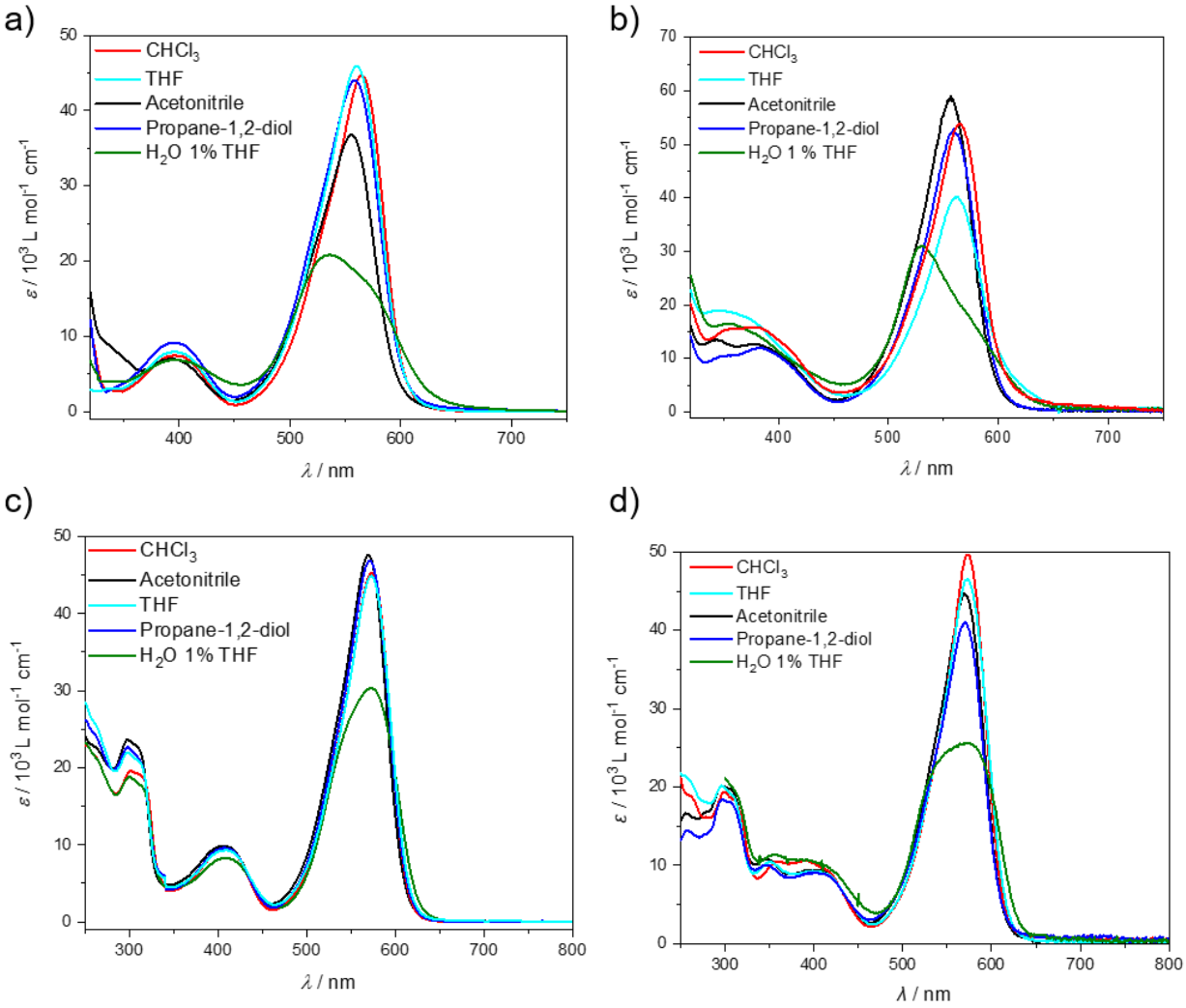

Figure S12. Solvent-dependent UV-Vis studies for **1** (a), **2** (b), **3** (c), **4** (d) at 298 K (*c* = 20 μM).

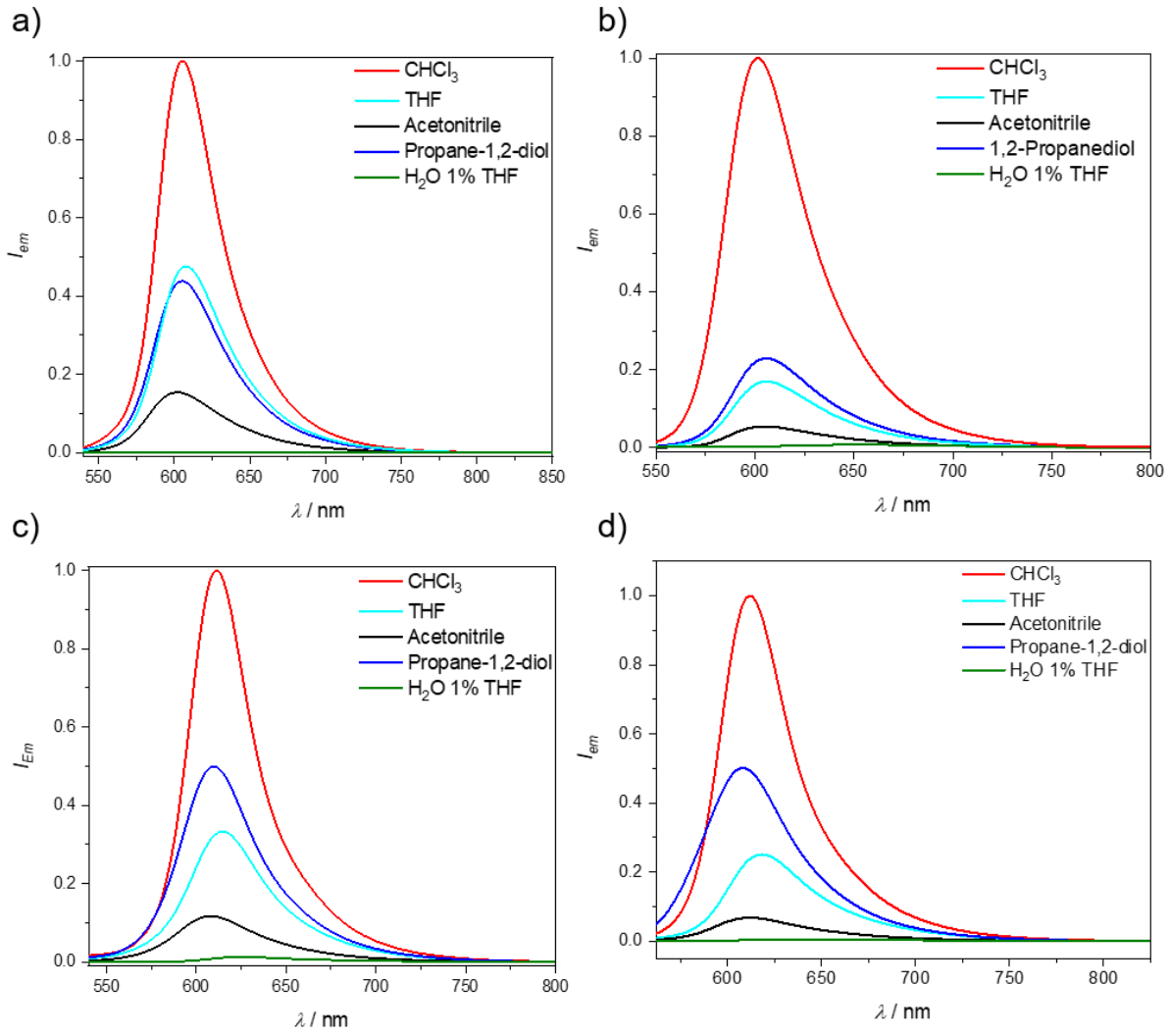

Figure S13. Solvent-dependent emission spectra of **1** (a), **2** (b), **3** (c), **4** (d) at 298 K (c = 20 μM). Excitation wavelength λ = 530 nm was applied for all measurements.

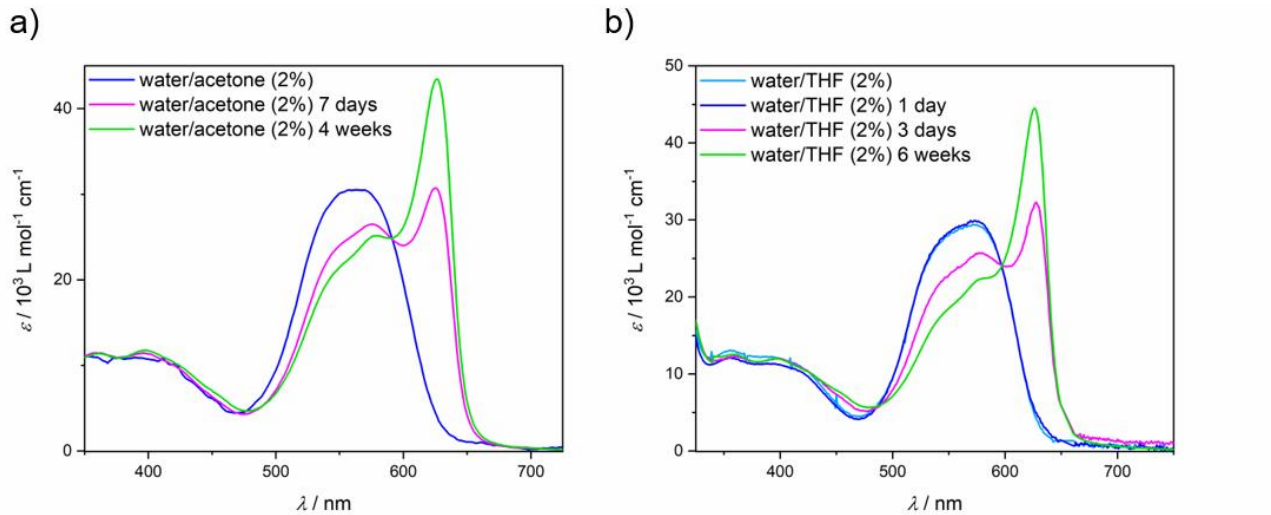

Figure S14. Time-dependent UV-Vis studies for **4** at 298 K (c = 20 μM) in aqueous media with the use of different co-solvents: acetone (a) and THF (b).

It has to be highlighted that this rearrangement process is occurring with several co-solvents (Figure S14a,b). The polarity and ratio of co-solvent is important for controlling the dynamics and the transformation time of this system, which enabled us to slow down the rearrangement process **4A** → **4B** over six weeks. These experiments also suggest the absence of hemiacetal or acetal formation by reaction of the aldehyde group with propane-1,2-diol, since the pathway complexity occurs in multiple solvents that are unable to react with the aldehyde group (for example THF and acetone, see Figure S14).

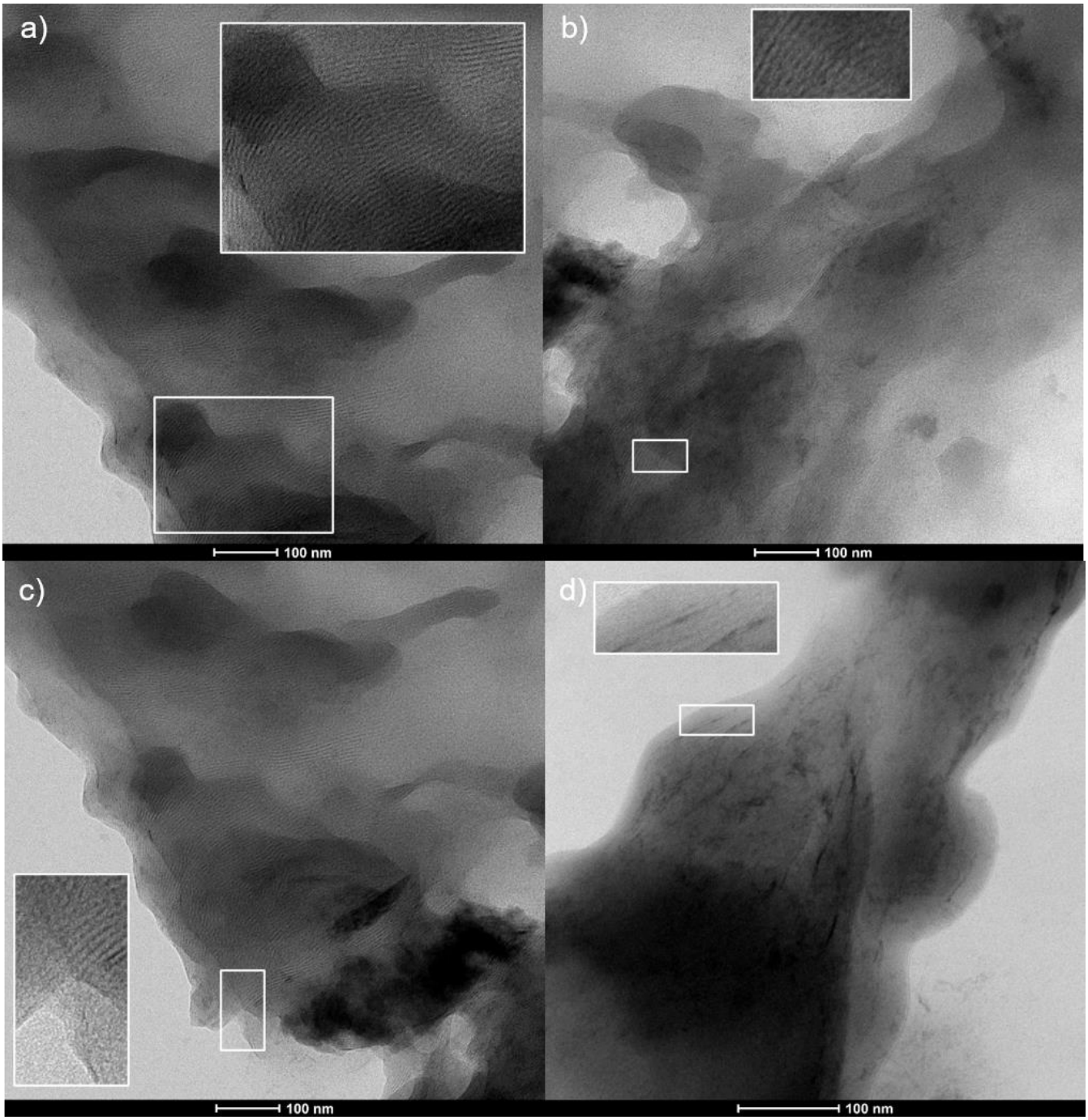

Figure S15. Conventional TEM studies of **1** in propane-1,2-diol/water (4/6, *c* = 20 μM). Samples were prepared by drop-casting aggregate solutions on a carbon-coated copper grid. Negative staining (uranyl acetate) was used for increased contrast.

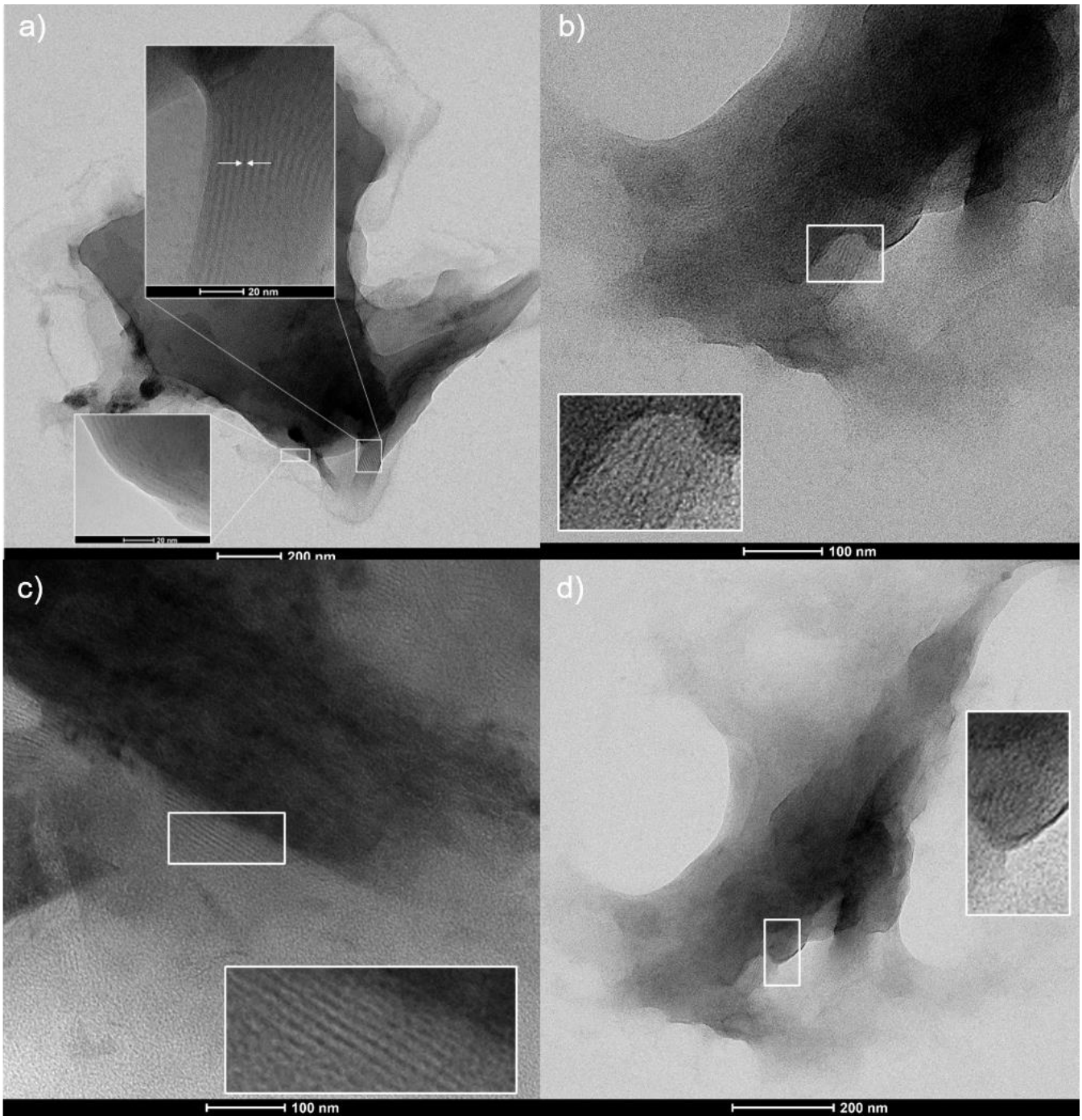

Figure S16. Conventional TEM studies of **2** in propane-1,2-diol/water (4/6, *c* = 20 μM). Samples were prepared by drop-casting aggregate solutions on a carbon-coated copper grid. Negative staining (uranyl acetate) was used for increased contrast.

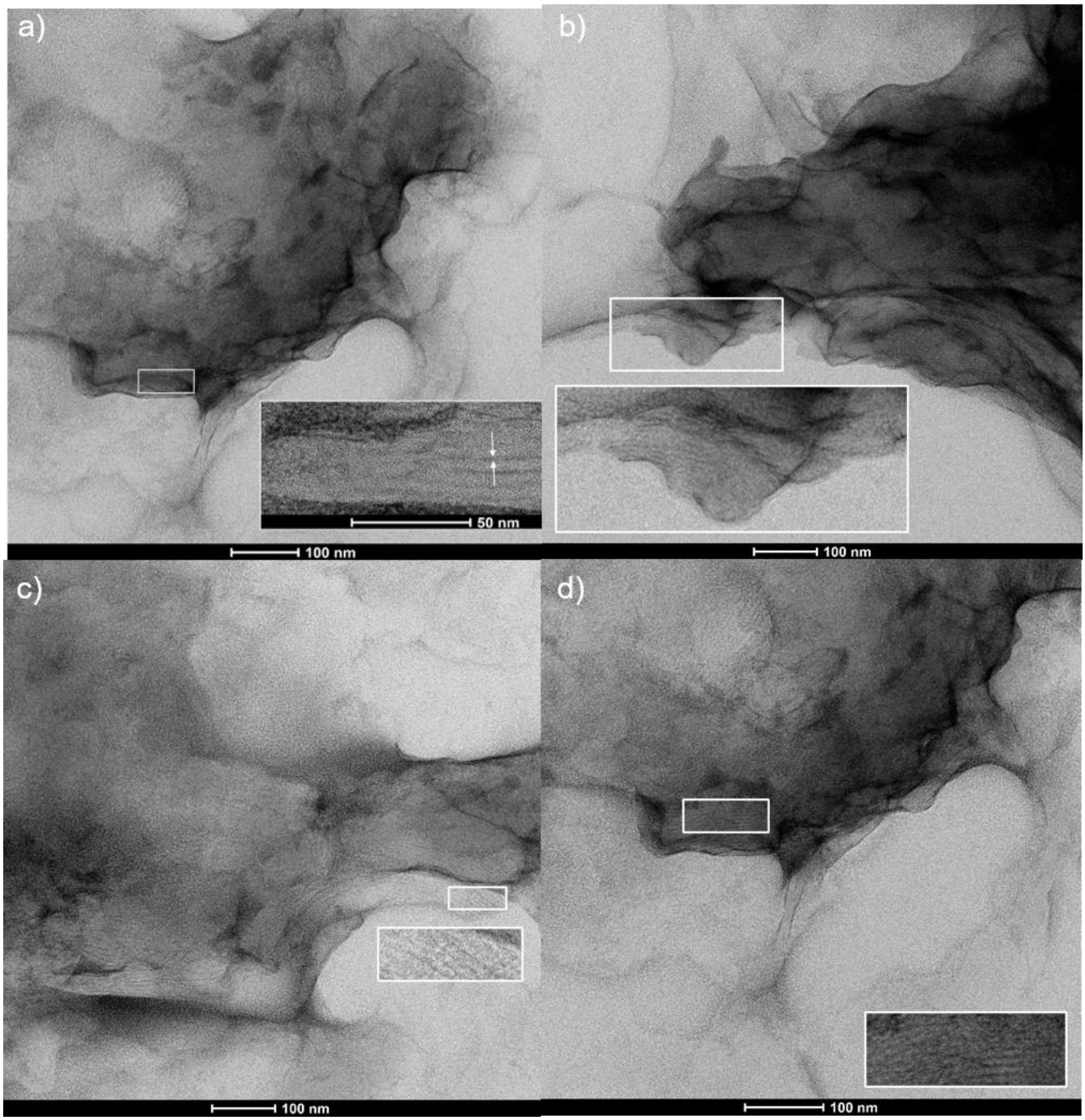

Figure S17. Conventional TEM studies of **3** in propane-1,2-diol/water (4/6, *c* = 20 μM). Samples were prepared by drop-casting aggregate solutions on a carbon-coated copper grid. Negative staining (uranyl acetate) was used for increased contrast.

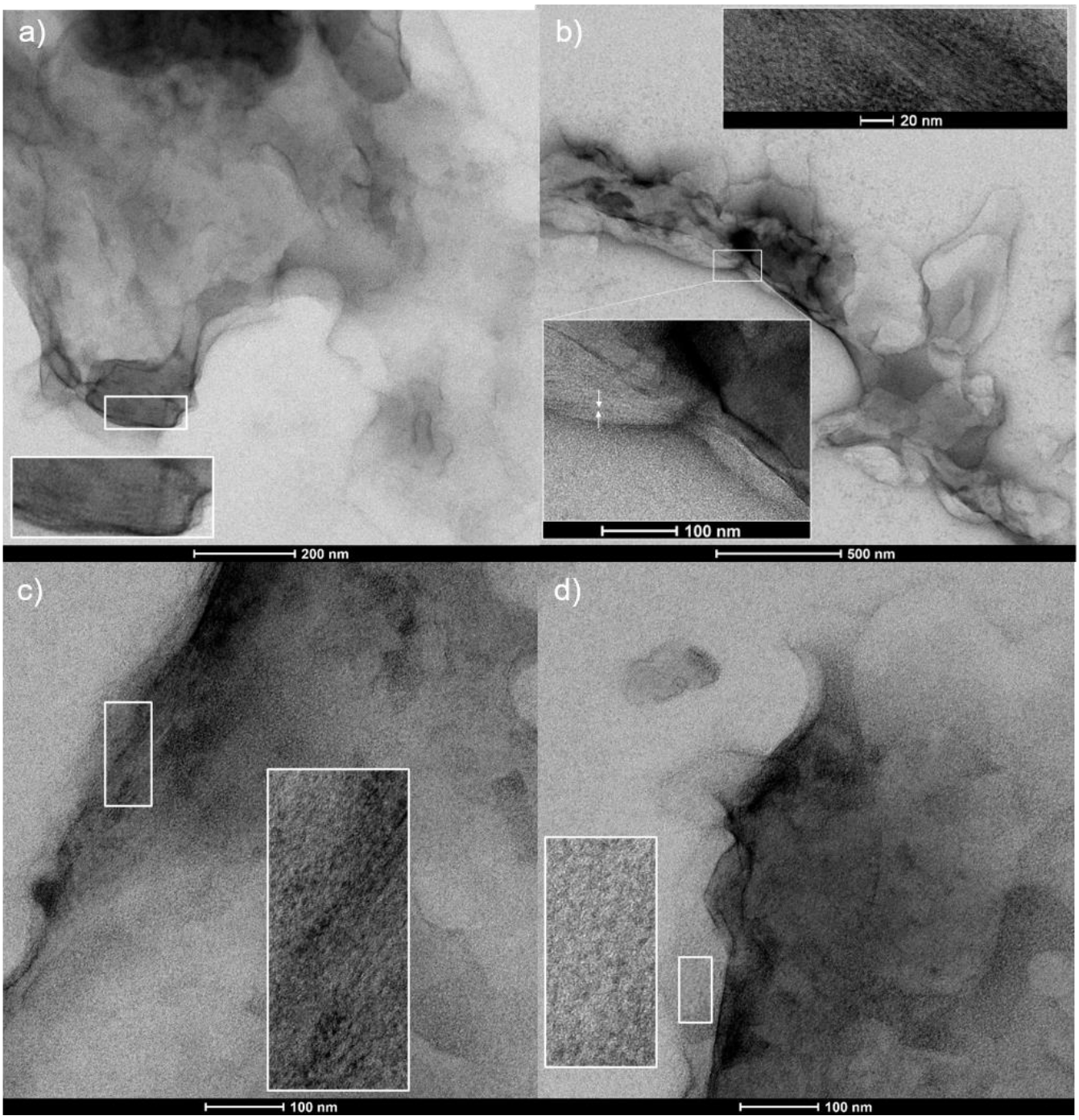

Figure S18. Conventional TEM studies of **4A** in propane-1,2-diol/water (4/6, *c* = 20 μM). Samples were prepared by drop-casting aggregate solutions on a carbon-coated copper grid. Negative staining (uranyl acetate) was used for increased contrast.

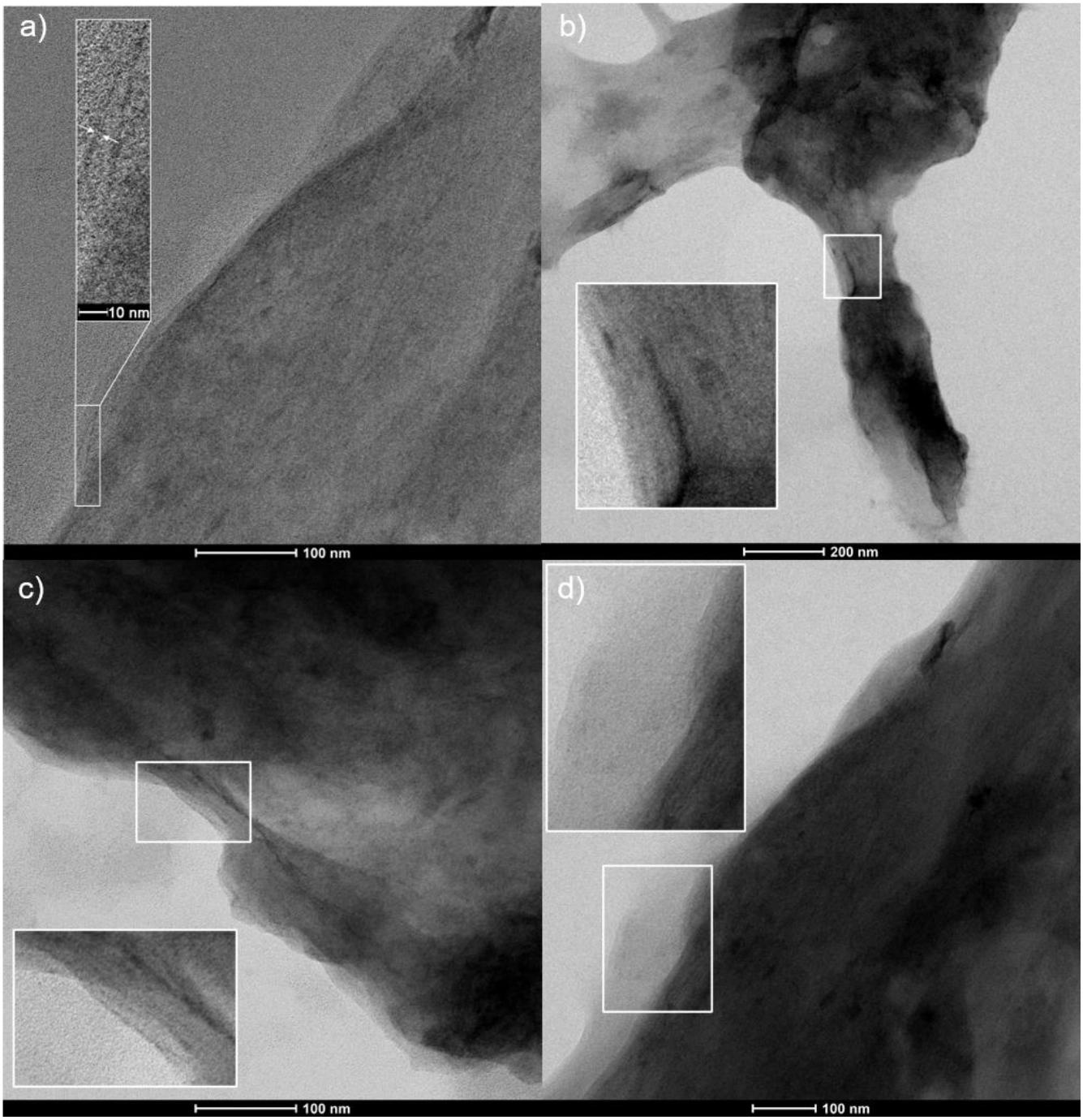

Figure S19. Conventional TEM studies of **4B** in propane-1,2-diol/water (4/6, *c* = 20 μM). Samples were prepared by drop-casting aggregate solutions on a carbon-coated copper grid. Negative staining (uranyl acetate) was used for increased contrast.

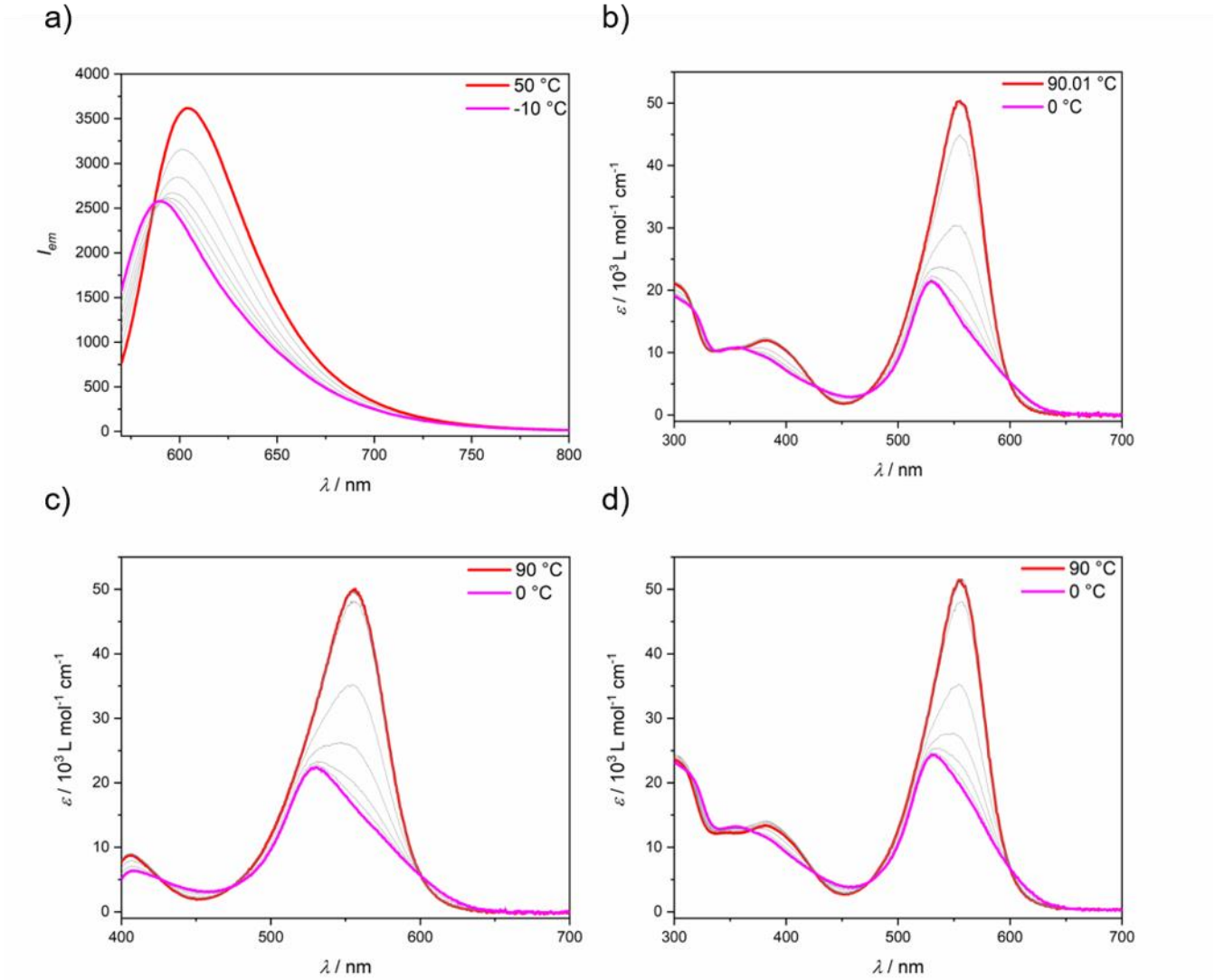

Figure S20. VT emission (a) and VT UV-Vis (b-d) studies of **2** in propane-1,2-diol/water (4/6) at 298 K, with a concentration and ramp rate of a) *c* = 20 μM, 2.0 K/min b) *c* = 10 μM, 0.1 K/min c) *c* = 10 μM, 10 K/min and d) *c* = 30 μM, 2 K/min.

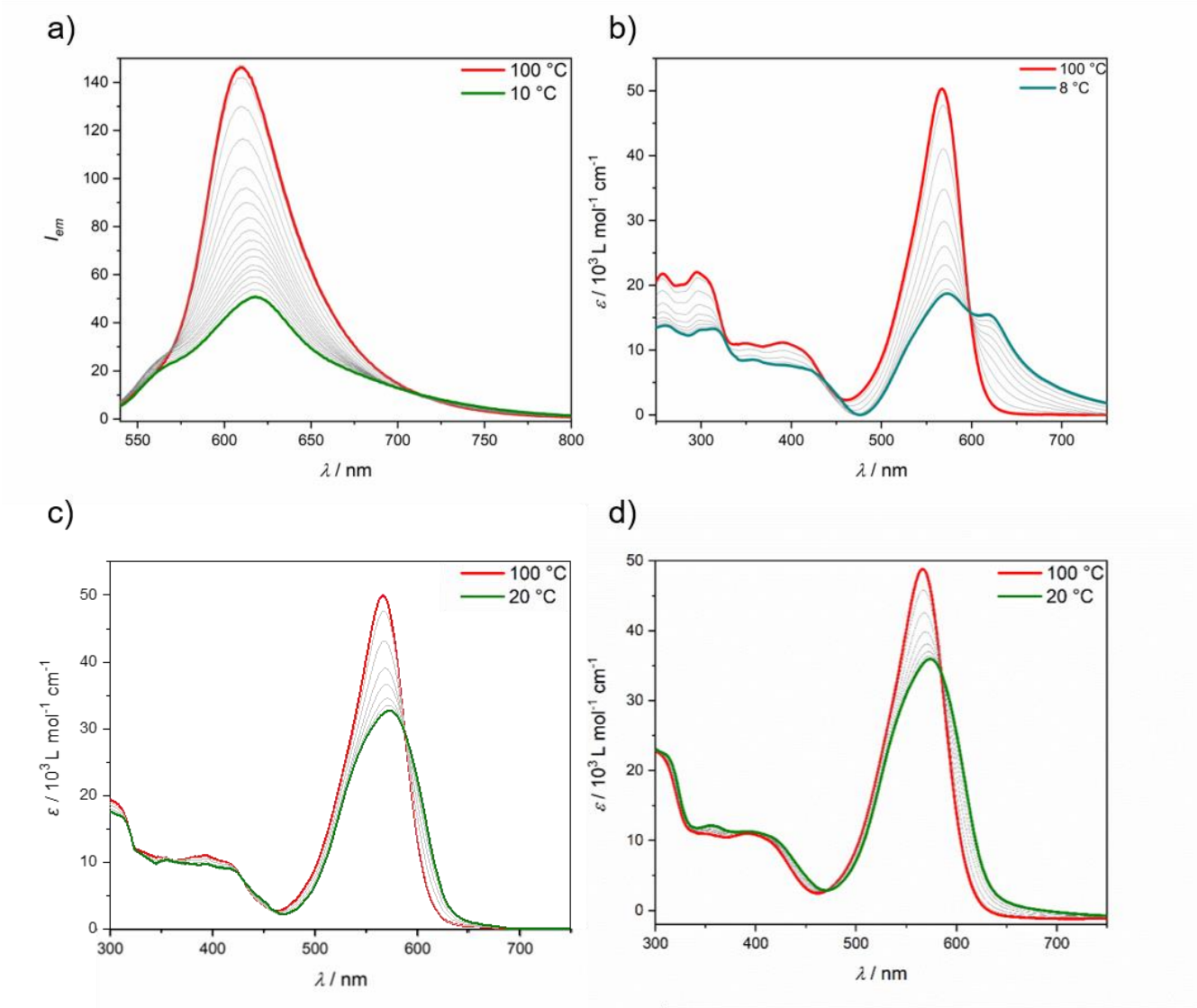

Figure S21. VT emission (a) and VT UV-Vis (b-d) measurements of **4A** in propane-1,2-diol/water (4/6) at 298 K, with a concentration and ramp rate of a) *c* = 20 μM, 10.0 K/min b) *c* = 20 μM, 0.1 K/min c) *c* = 10 μM, 10 K/min and d) *c* = 30 μM, 10 K/min.

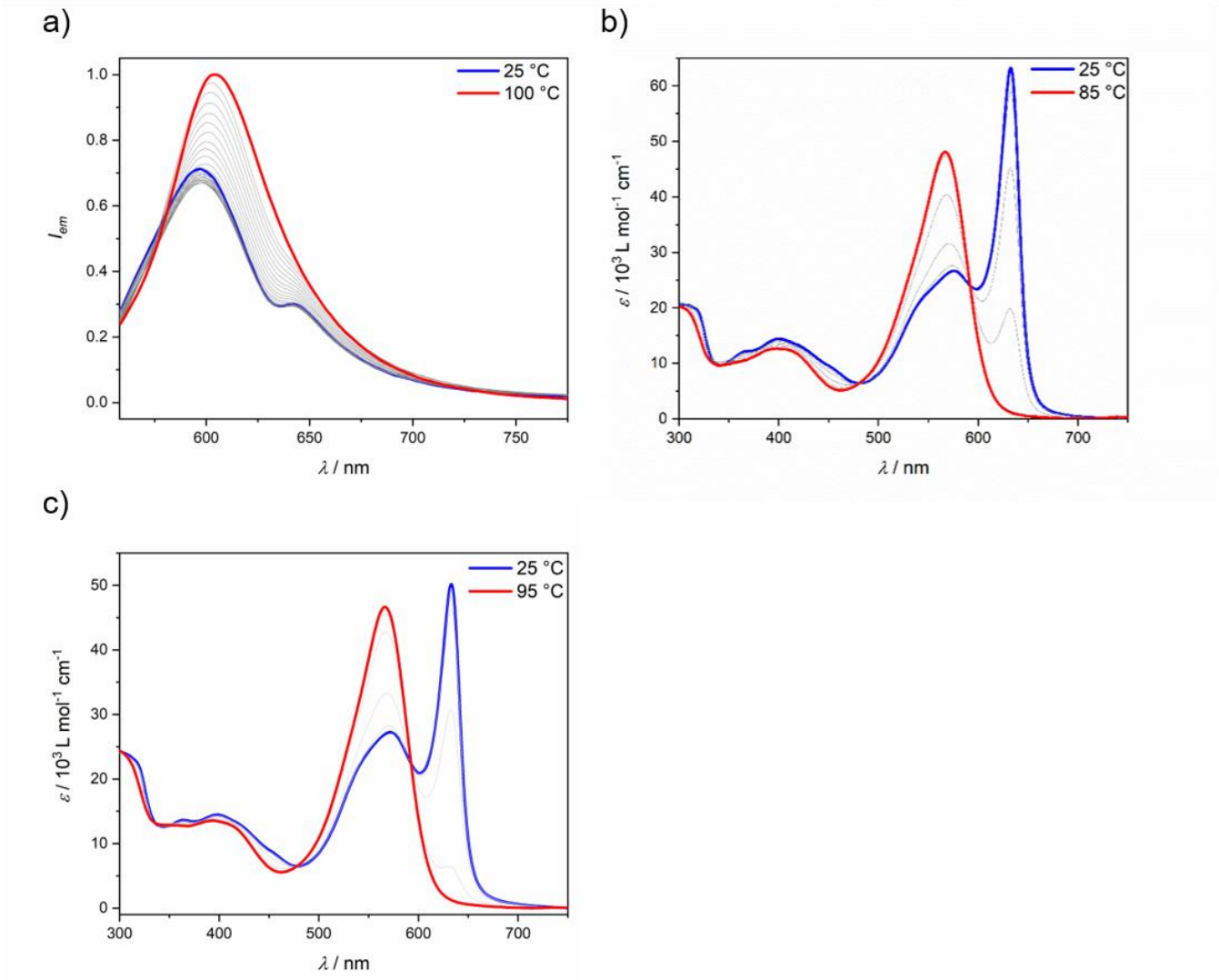

Figure S22. VT emission (a) and VT UV-Vis (b-d) studies of **4B** in propane-1,2-diol/water (4/6) at 298 K, with a concentration and ramp rate of a) *c* = 20 μM, 2.0 K/min b) *c* = 10 μM, 2.0 K/min c) *c* = 30 μM, 2.0 K/min.

VT emission studies exhibit the quenching of emission intensities upon aggregation for all investigated species (Figure S20-22). The comparison of species **4A** and **4B** unveil higher emission intensities for the latter in the final aggregated state, which is in line with an emission enhancement upon J-type aggregation.

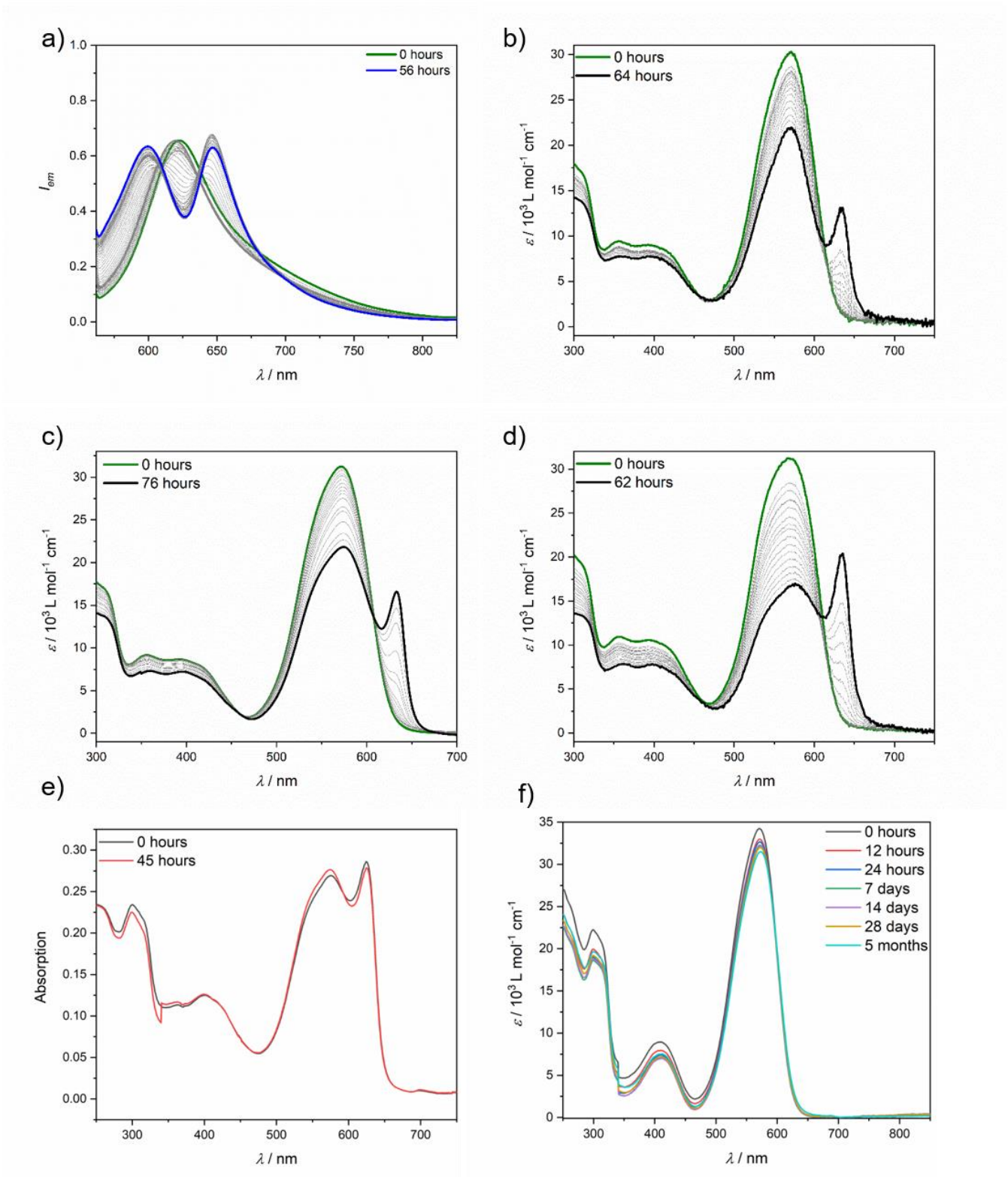

Figure S23. Time-dependent emission (a) and UV-Vis (b-d) studies of transformation of **4A** to **4B** in propane-1,2-diol/water (4/6) at 298 K a concentration of a) c = 50 μM, b) c = 20 μM, c) c = 30 μM, d) c = 40 μM. e) Time dependent UV-Vis changes upon mixing **4A** and **3** in a 1:1 ratio at 298 K with a c = 20 μM. f) Time dependent UV-Vis changes of **3** at 298 K with a c = 20 μM.

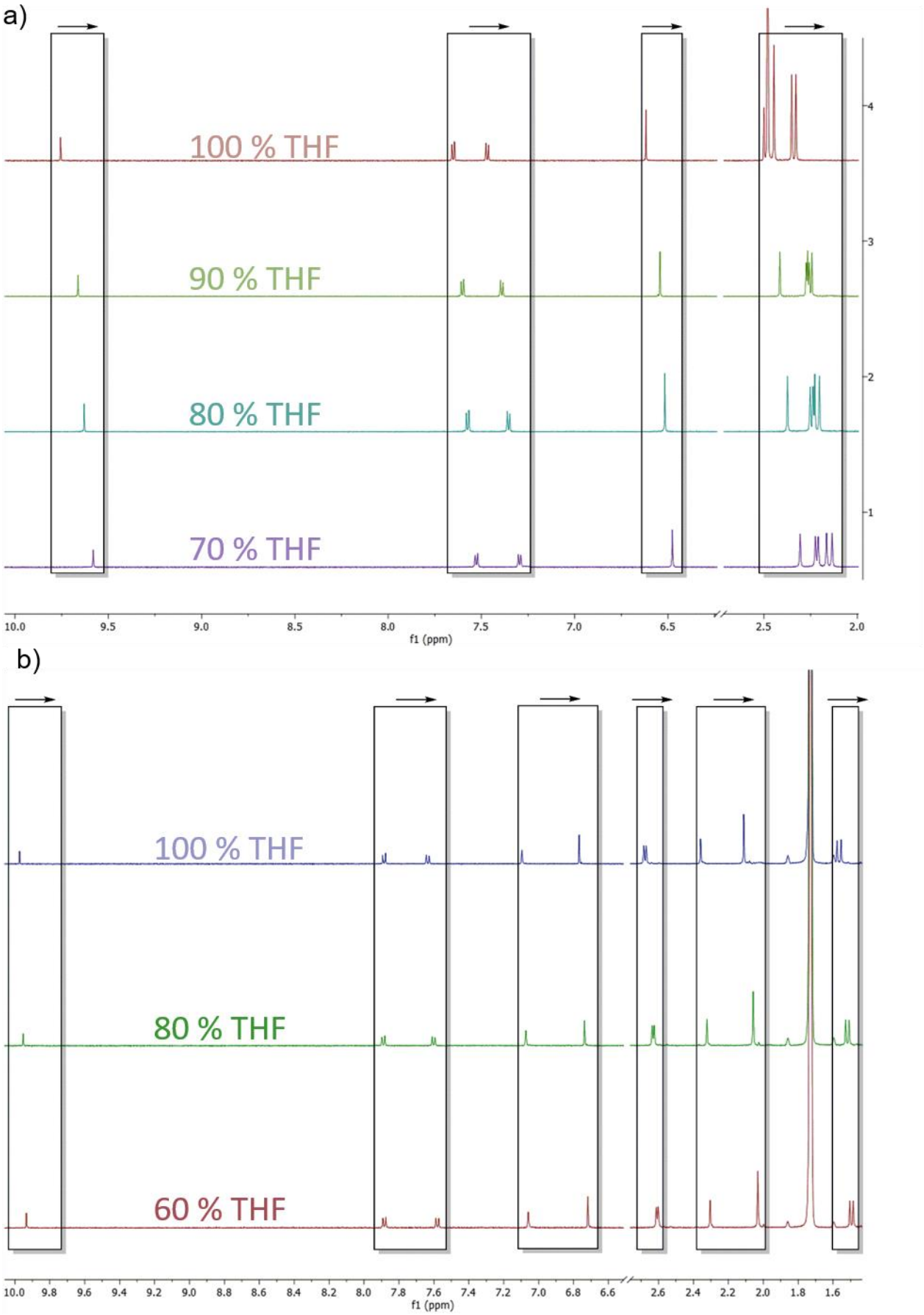

Figure S24. ^{1}H NMR spectra of **2** (a) and **4** (b) (c = 1 mM and 298 K) at different ratios of D_2O/THF-d_8.

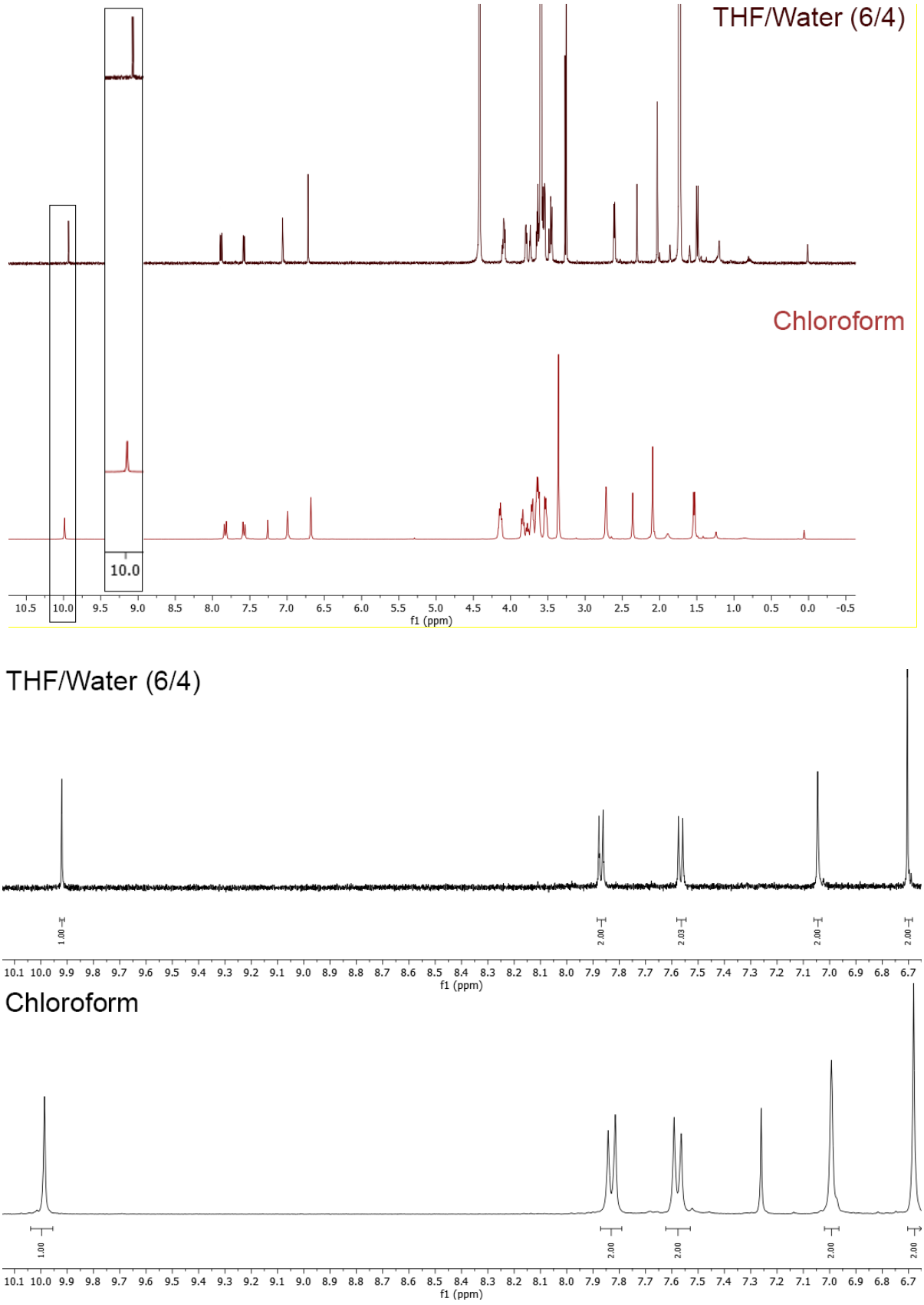

Figure S25. Comparison of the ^{1}H NMR spectra of **4** (1 mM, 298 K) in $CDCl_3$ and THF-d_8/D_2O (6:4). Top: full spectra; bottom: magnified aromatic region.

The ^{1}H NMR spectra in both media exhibit a clear aldehyde resonance at ~10 ppm. The integration of the NMR signals in both media is in accordance with the formation of a single species, i.e. aldehyde. Moreover, the lack of additional NMR signals corresponding to the proton of the hydrate form (i.e. at ca. 5 ppm) in aqueous solutions suggests that the hydrate form is present, if at all, in trace amounts.

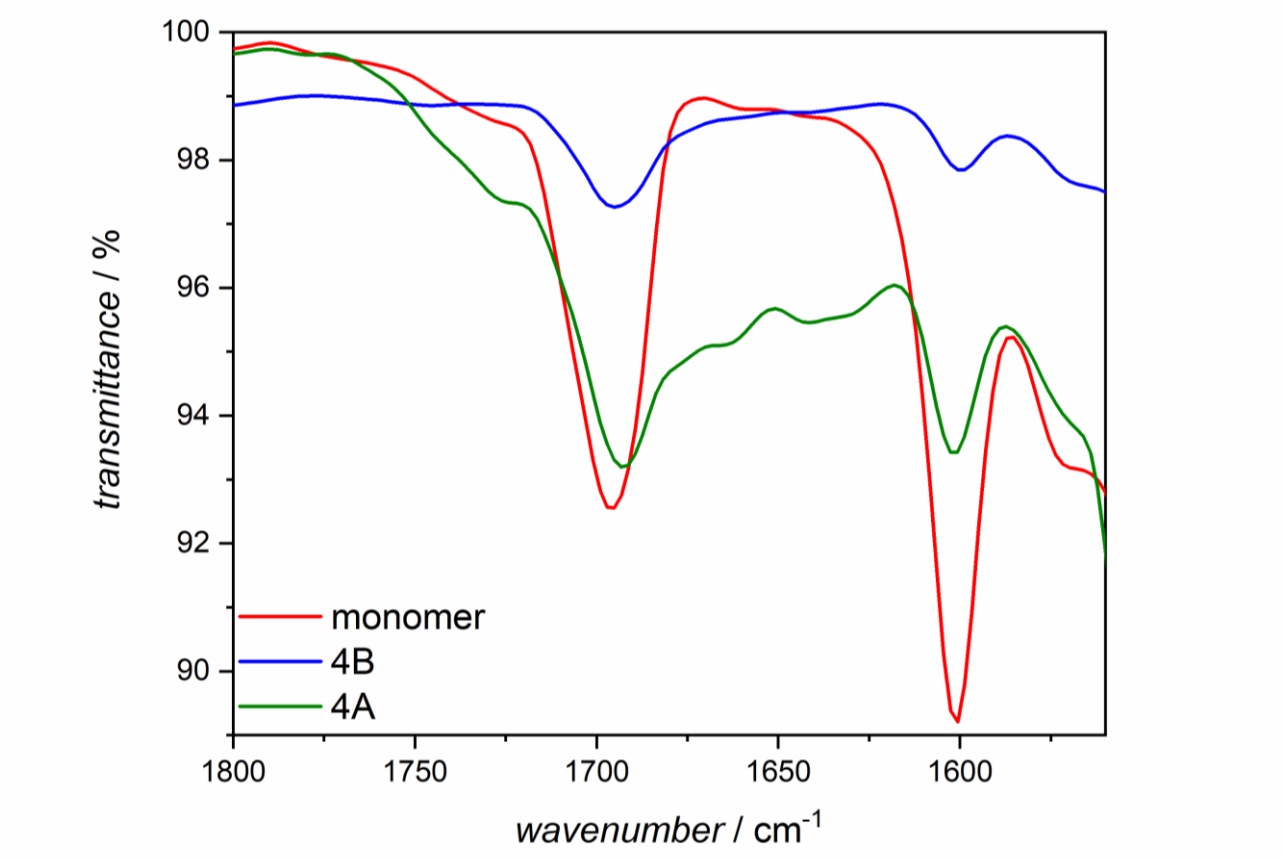

Figure S26. FTIR spectra of compound **4**: monomer in $CHCl_3$ (1 mM) and aqueous solutions (1% THF) of aggregates **4A**, **4B** 8 K and 1 mM.

FTIR studies of compound **4** in $CHCl_3$ unravel the existence of characteristic non-hydrogen-bonded carbonyl stretching aldehyde band at 1695 cm^{-1}. Also, for the aggregated species, a closer look in the carbonyl stretching region exhibit sharp carbonyl stretching bands with almost no shift with respect to the monomeric species (**4A**: 1693 cm^{-1}, **4B**: 1695 cm^{-1}), which underlines that hydrogen bonding interactions between the aldehyde functions play a less prominent role in the self-assembly of **4**.

On the other hand, the dipole-dipole repulsion of this aldehyde is very important for destabilizing kinetic species **4A** and inducing the formation of thermodynamic **4B**, since compound **3**, which lacks an aldehyde group, does not show any transformation in an experimentally observable time span.

References

[1] A. Rödle, B. Ritschel, C. Mück-Lichtenfeld, V. Stepanenko, G. Fernández, *Chem. Eur. J.* **2016**, *22*, 15772.
[2] L. Bucher, S. M. Aly, N. Desbois, P.-L. Karsenti, C. P. Gros, P. D. Harvey, *J. Phys. Chem. C 2017*, *121*, 6478.
[3] F. A. Mandl,V. C. Kirsch,I. Ugur,E. Kunold, J. Vomacka,C. Fetzer,S. Schneider,K. Richter,T. M. Fuchs,I. Antes and S. A. Sieber, *Angew. Chem. Int. Ed.* **2016**, *55*, 14852 –14857.
[4] M. Korzec, S. Kotowicz, K. Laba, M. Lapkowski, J. G. Malecki, K. Smolarek, S. Maćkowskian, E. Schab-Balcerzak, *Eur. J. Org. Chem.* **2018***,* 1756–1760.
[5] S. Chen, X. Huang, S. Decurtins, C. Albrecht, S. Liu, *Polyhedron* **2017**, *134*, 287–294.
[6] H. M. M. Ten Eikelder, A. J. Markwoort, T. F. A. De Greef, P. A. J. Hilbers, *J. Phys. Chem. B* **2012**, *116*, 5291-5301.
[7] A. J. Maarkvort, H. M. M. Ten Eikelder, P. J. J. Hilbers, T. F. A. De Greef, E. W. Meijer, *Nat. Commun.* **2011**, *2*, 509-517.